Soft Matter

REVIEW

Cite this: *Soft Matter*, 2015, 11, 9229

Recent advances in clay mineral-containing nanocomposite hydrogels

Li Zhi Zhao,[a] Chun Hui Zhou,*[abc] Jing Wang,[c] Dong Shen Tong,[a] Wei Hua Yu[a] and Hao Wang*[c]

Received 25th May 2015,
Accepted 15th September 2015

DOI: 10.1039/c5sm01277e

www.rsc.org/softmatter

Clay mineral-containing nanocomposite hydrogels have been proven to have exceptional composition, properties, and applications, and consequently have attracted a significant amount of research effort over the past few years. The objective of this paper is to summarize and evaluate scientific advances in clay mineral-containing nanocomposite hydrogels in terms of their specific preparation, formation mechanisms, properties, and applications, and to identify the prevailing challenges and future directions in the field. The state-of-the-art of existing technologies and insights into the exfoliation of layered clay minerals, in particular montmorillonite and LAPONITE®, are discussed first. The formation and structural characteristics of polymer/clay nanocomposite hydrogels made from *in situ* free radical polymerization, supramolecular assembly, and freezing–thawing cycles are then examined. Studies indicate that additional hydrogen bonding, electrostatic interactions, coordination bonds, hydrophobic interaction, and even covalent bonds could occur between the clay mineral nanoplatelets and polymer chains, thereby leading to the formation of unique three-dimensional networks. Accordingly, the hydrogels exhibit exceptional optical and mechanical properties, swelling–deswelling behavior, and stimuli-responsiveness, reflecting the remarkable effects of clay minerals. With the pivotal roles of clay minerals in clay mineral-containing nanocomposite hydrogels, the nanocomposite hydrogels possess great potential as superabsorbents, drug vehicles, tissue scaffolds, wound dressing, and biosensors. Future studies should lay emphasis on the formation mechanisms with in-depth insights into interfacial interactions, the tactical functionalization of clay minerals and polymers for desired properties, and expanding of their applications.

1. Introduction

Hydrogels commonly refer to a class of soft matter consisting of a three-dimensional cross-linked network of hydrophilic insoluble polymers (hydrogelators) with water as the dispersion medium.[1] With a significant amount of water in the network, hydrogels exist in a half liquid-like and a half solid-like state[2] and thereby possess high water storage capacity, elasticity, flexibility, and permeability.[3] The network structure in the hydrogels can be formed by either chemical cross-linking or physical cross-linking.[4] The physically cross-linked hydrogels are formed through microcrystallization or the entanglement of polymer chains with noncovalent bonds, including electrostatic interaction, hydrophobic interaction, hydrogen bonding, and coordination bonds. Scientific studies have proved that hydrogels can also be produced from the supramolecular assembly of amphiphilic organic molecules[5] or inorganic nanoparticles[6] in water. Some physical hydrogels can undergo a sol–gel phase transition (SGPT)[7] as a response to external stimuli.[8,9] In contrast, the chemically cross-linked hydrogels are permanent networks formed through covalent bonds, enabling volume phase transitions (VPT)[10] when exposed to external physical or chemical stimuli, including temperature,[11,12] light, electric field,[13] ionic strength,[14] pH,[15] enzyme,[16] and biomolecules. As a result of these characteristics, hydrogels can be used as superabsorbents,[17,18] packaging materials,[19] soft lenses,[20] microfluidic devices,[21] catalyst supports,[22,23] biomedical materials,[24,25] and bioactuators[26] (Fig. 1a).

Hydrogel-forming insoluble polymers or amphiphilic organic molecules and inorganic nanoparticles can be assembled to form nanocomposite hydrogels. One of the most frequently used types of nanoplatelets (NPs) are two-dimensional (2D) nanomaterials, such as layered clay mineral nanoplatelets (CNPs)[27,28]

[a] *Research Group for Advanced Materials & Sustainable Catalysis (AMSC), Institute of Advanced Catalytic Materials, State Key Laboratory Breeding Base of Green Chemistry-Synthesis Technology, College of Chemical Engineering, Zhejiang University of Technology, Hangzhou 310032, China. E-mail: clay@zjut.edu.cn, chc.zhou@aliyun.com; Tel: ++86 135 8806 6098*

[b] *Key Laboratory of Clay Minerals of Ministry of Land and Resources of The People's Republic of China, Engineering Research Center of Non-metallic Minerals of Zhejiang Province, Zhejiang Institute of Geology and Mineral Resource, Hangzhou 310007, China*

[c] *Centre of Excellence in Engineered Fibre Composites, University of Southern Queensland, Toowoomba, Queensland 4350, Australia. E-mail: Chun.Zhou@usq.edu.au*

and layered double hydroxide (LDH) nanosheets.[29] Due to the significant effects of CNPs on the structure and properties of polymer/CNPs nanocomposite hydrogels, such nanocomposite hydrogels have attracted particular attention over the past decade or so, as demonstrated by the rapid growth in the number of relevant scientific publications (Fig. 1b). Smectitic clay minerals (Fig. 2), in particular natural montmorillonite and synthetic hectorite (*e.g.*, LAPONITE®), are often used primarily due to their layered structure and unique properties. Each TOT layer of the clay minerals consists of one Al–O or Mg–O octahedral (O) sheet sandwiched by two Si–O tetrahedral (T) sheets, with negative charges that arise mainly from partial isomorphous substitution, typically Al^{3+} by Mg^{2+} in montmorillonite and Mg^{2+} by Li^{+} in hectorite in the octahedral sheet.[27,28] For this reason, exchangeable cations such as Na^{+} exist in the interlayer space. Such a form of structure endows these clay minerals with outstanding cation exchangeability, adsorption and swellability. Importantly, these layered clay minerals can be fine-exfoliated to yield nanoplatelets[30] with a high aspect ratio (*e.g.*, approximately $100 \times 100 \times 1$ nm^3 for montmorillonite[31]). Though such exfoliated clay minerals in water can form a physically cross-linked hydrogel, this unique feature of polymer/clay mineral nanocomposite hydrogels received little attention, until 2002 when a pioneering study from Haraguchi and Takehisa[32] unveiled a unique poly(*N*-isopropyl acrylamide) (PNIPAM)/clay mineral nanocomposite hydrogel. The nanocomposite hydrogel exhibited extraordinary mechanical, optical, and swelling/deswelling properties. Since then, a variety of clay mineral-containing nanocomposite

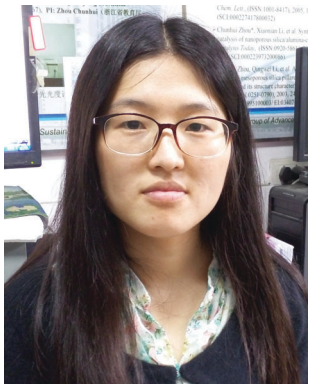

Li Zhi Zhao

Li-Zhi Zhao is currently a research (academic) postgraduate under the supervision of Prof. Chun-Hui ZHOU at the Research Group for Advanced Materials & Sustainable Catalysis (AMSC), the Institute of Advanced Catalytic Materials, Zhejiang University of Technology (ZJUT), Hangzhou, China. She received her Bachelor's Degree in Chemical Engineering from Hebei Normal University of Science and Technology. Her research presently centers on the preparation of advanced clay-based materials, hydrogels and related nanostructured catalysts and their potential for the catalytic conversion of biochemicals into value-added products.

Chun Hui Zhou

Dr Chun-Hui (Clayton) Zhou, born and brought up in Miaoqian, Qingyang, Anhui, is Professor of Chemical Engineering and Leader of the Research Group for Advanced Materials and Sustainable Catalysis (AMSC), Zhejiang University of Technology. He is Adjunct Professor of University of Southern Queensland and Editorial Member of Applied Clay Science (Elsevier) and Journal Porous Materials (Springer). He has worked as a visiting academic at the University of Queensland (2006–2007) and as a visiting professor at the University of Western Australia (2010). His R&D focuses on advanced clay materials, hydrogels, and the catalytic conversion of biochemicals and biomass. He also teaches industrial catalysis, materials science and science literacy.

Jing Wang

Dr Jing Wang, Research Fellow, has a broad research interest in natural and synthetic functional polymers, biocomposites and bioresins, and the electrospinning of nanofibers. His key interests include the electrospinning of thermos-responsive hydrogel nanofibers and hemp-reinforced PLA composites with antibacterial performance. He has been awarded and/or involved in more than 10 projects, including Cooperative Research Centre for Advanced Composite Structures (CRC-ACS, Australia), Research in Business (RiB, Australia) and Forest and Wood Products Australia (FWPA). He has obtained more than 50 academic publications and is currently a supervisor of three PhD candidates.

Dong Shen Tong

Dr Dong Shen Tong is Associate Professor of the College of Chemical Engineering, Zhejiang University of Technology, China. He obtained his PhD degree (2008) from Chengdu Institute of Organic Chemistry, Chinese Academy of Sciences. Since August 2008, he has been working at the Research Group for Advanced Materials and Sustainable Catalysis (AMSC), the Institute of Advanced Catalytic Materials, at Zhejiang University of Technology. His research interests are in advanced materials and heterogeneous catalysis, and clay-based materials and their application in sustainable catalysis.

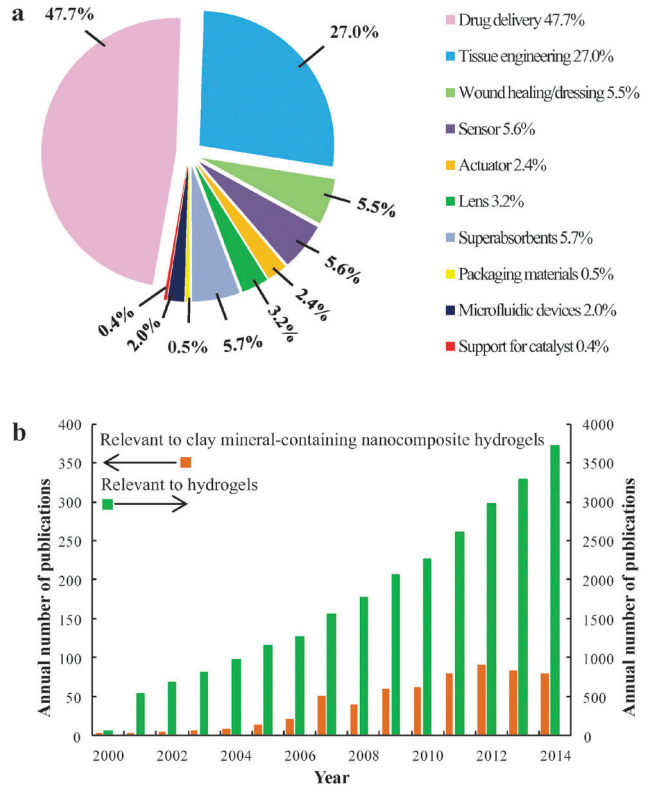

Fig. 1 (a) Application category distribution of hydrogels (by percentage) according to peer-reviewed scientific papers published (from 2000 to end of 2014) relating to the topic of hydrogels. (b) Annual number of peer-reviewed papers published (from 2000 to 2014) relevant to the topics of hydrogels and clay mineral-containing nanocomposite hydrogels. (Data from Web of Science™ Core Collection. Search terms: hydrogels and clay.)

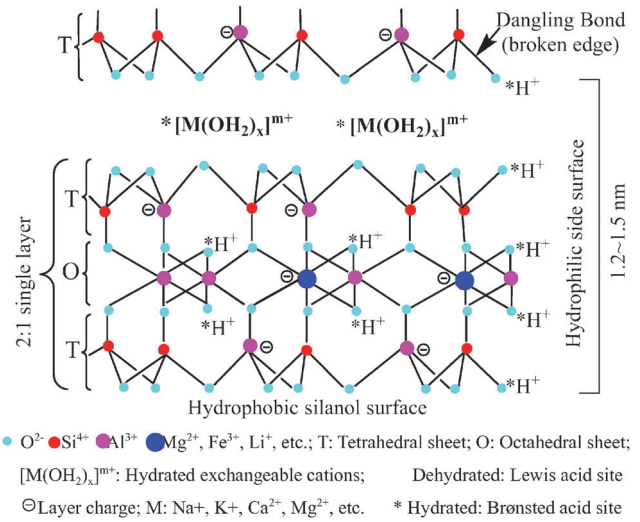

Fig. 2 Schematic drawing of the structure of the frequently used 2 : 1-type (TOT-type) layered smectite minerals in nanocomposite hydrogels. Each layer consists of an octahedral alumina/magnesia sheet sandwiched by two tetrahedral sheets of silica through sharing –O–. Neighboring layers are loosely bound with counterions (typically sodium or calcium) in the interlayer space. The interlayer space is the space between adjacent layers. In the presence of water, the counter-ions undergo hydration, causing the clay mineral to expand and delaminate.

hydrogels have been reported. These studies indicated that when such 2D CNPs are added to a polymeric hydrogel matrix, additional interactions take place between CNPs and polymers, resulting in the creation of nanocomposite hydrogels with improved mechanical properties,[33–35] stimuli-responsiveness,[36,37] swellability,[38] and self-healing abilities,[39] compared to hydrogels consisting of single hydrophilic polymers.

This paper intends to review and analyze recent advances in clay mineral-containing nanocomposite hydrogels with an objective to highlight the state-of-the-art technologies used in the preparation of clay mineral-containing nanocomposite hydrogels. Another objective of this paper is to examine the current understanding of the effects of clay mineral additives

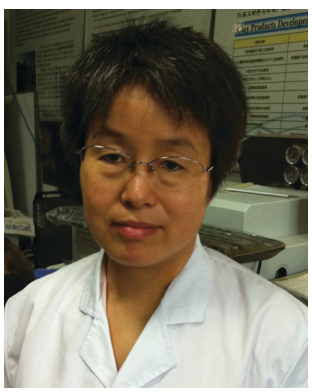

Wei Hua Yu

Dr Wei Hua Yu is Professor of Chemical Engineering and a member of the Research Group for Advanced Materials and Sustainable Catalysis, the Institute of Advanced Catalytic Materials, at Zhejiang University of Technology (ZJUT), China. She received her PhD (2007) from ZJUT, China. She worked as a visiting scholar at the Department of Chemistry in Michigan State University, USA, in 2005. Her research interests are in advanced clay-based functional materials, layered and mesostructured materials, sol–gel chemistry, and nanostructured catalysts and their applications in catalysis and environmental treatment such as in the catalytic conversion of biomass into liquid fuels and chemicals.

Hao Wang

Dr Hao Wang, Professor and Director of the Centre of Excellence in Engineered Fibre Composites at USQ, received his PhD in materials science and engineering from the University of Queensland in 2001, and has been working at University Southern Queensland since 2006. His research interests cover metals, ceramics, and hydrogels. Currently his research focuses on biomass composites, green concrete, and nanomaterials. He has published 7 books, 4 book chapters and 140 journal papers. His papers were ranked by Science Direct as the 1st, 5th, and 9th of the top 25 articles for the journal Composites Part B: Engineering for 2014.

on polymer/clay hydrogel network formation, their properties, and applications. The third objective is to identify the existing challenges that may steer future studies in this field. Therefore, in the present paper, first, the exfoliation of layered clay minerals is overviewed. Then, the formation of polymer/clay mineral nanocomposite hydrogels and their inherent interactions in the network are discussed. Next, the characteristics of the clay mineral-containing nanocomposite hydrogels in regard to their optical and mechanical properties, swelling–deswelling behavior, and stimuli-responsiveness are analyzed, with a particular focus on the effects of clay mineral nanoplatelets on these properties. Subsequently, the performance of hydrogels and their potential applications as superabsorbents and biomaterials are evaluated with respect to the specific constituent clay minerals. Finally, the existing problems and prospects in this field are discussed.

2. Insights into the formation of nanocomposite hydrogels

2.1 Exfoliation and addition of clay minerals into polymeric hydrogel networks

Two-dimensional CNPs can act as multifunctional cross-linkers[40,41] or fillers[42] in nanocomposite hydrogels. As far as the role of clay minerals as an enhancement nanophase in nanocomposite hydrogels is concerned, to obtain and utilize CNPs from the exfoliation of clay mineral tactoids is a critical issue. For most clay minerals, due to their greater layer charge densities (*e.g.*, vermiculite, 1.1–2.0 electronic charges per unit cell) or electrically neutral layers (*e.g.*, kaolinite), exfoliation is difficult. In contrast, montmorillonite and LAPONITE® are composed of several parallel TOT layers, and the negative charge per unit cell from isomorphic substation ranges between 0.5 and 1.3 electronic charges. Their parallel TOT layers, which are usually packed one above the other with exchangeable hydrated cations located between the layers, can be effectively exfoliated by proper treatment (Fig. 3). When water and polar organic molecules are attracted by exchangeable cations and are intercalated in the layers, the structure expands in a direction perpendicular to the layers.

For the delamination of layered montmorillonite and LAPONITE® to form exfoliated CNPs, the electrostatic forces between the negatively charged layer and interlayer cations must be overcome. In addition, the swelling of the layered structure depends heavily on the exchangeable cation or intercalated species in the interlayer space. Therefore, easily hydrated cations (*e.g.*, Na^+)[43] and bulky organic cations[44] are introduced into the interlayer space by an ion exchange reaction (Fig. 3a). Moreover, for an effective exfoliation, the use of a dilute aqueous suspension of clay minerals is imperative. Furthermore, the exfoliation process is usually conducted with the aid of sonication[45] and using exfoliating agents such as pyrophosphate[46] or polymeric species.[47] For example, Guimarães *et al.*[46] exfoliated LAPONITE® and obtained a transparent LAPONITE® suspension (20 g L^{-1}) by mixing 3.6 g of LAPONITE® with 180 mL of an aqueous solution of tetrasodium pyrophosphate (1 g L^{-1}) by stirring for 30 min. Mongondry *et al.*[48] revealed that tetrasodium pyrophosphate was adsorbed onto the positively charged edges and restrained the interaction between the edges and the negatively charged surfaces of the LAPONITE®, thereby hindering the reaggregation of exfoliated CNPs. In particular, the monomer, a precursor of the hydrogel-forming polymer, can be used to facilitate the exfoliation and to stabilize the CNPs.[49] Consequently, materials consisting of CNPs with a monomer can be directly used in the subsequent *in situ* free radical polymerization. The exfoliation and stabilization of CNPs can also be achieved with polymeric species such as polyethylene oxide (PEO)[48] or polyamine salts (Fig. 3b). For instance, Chu *et al.*[47] synthesized hydrophobic POP–AMO polyamines (POP: polyoxypropylene; AMO: amine-terminating Mannich oligomers) for Na^+-montmorillonite exfoliation. Such POP-segmented quaternary salts can undergo an ionic exchange reaction with Na^+ of montmorillonite and, consequently, expand the montmorillonite into the exfoliated CNPs. Recently, Wang *et al.*[50] also exfoliated pristine multilayered sodium montmorillonite into individual nanoplatelets

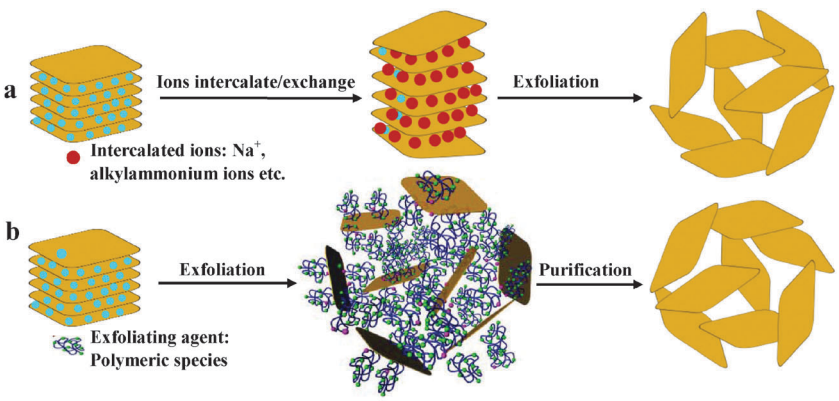

Fig. 3 Techniques for exfoliating clay minerals: (a) easily hydrated cations or bulky ion intercalation/exchange. Bulky cations can be intercalated in the interlayer space to cause the layered structure to swell and exfoliate; (b) using polymeric species as an exfoliating agent. These exfoliation processes are often used with the aid of sonication. Adapted and reprinted by permission from Macmillan Publishers Ltd; [Nature] (ref. 50), copyright (2013).

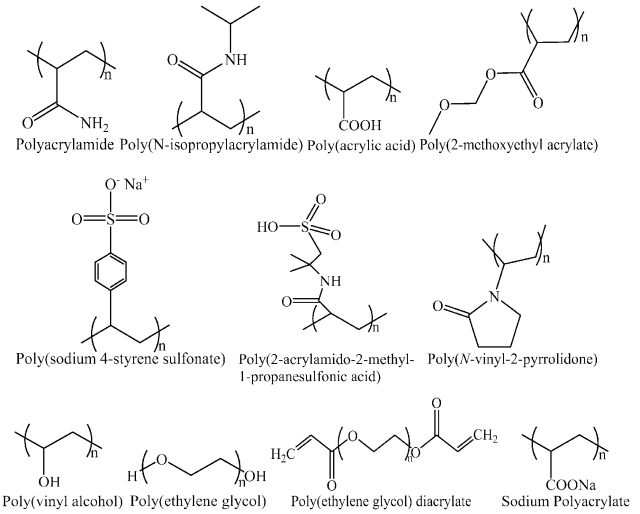

Fig. 4 Polymers frequently used in forming clay mineral-containing nanocomposite hydrogels.

using polyamine quaternary salts. The platelet-to-platelet multilayers of the montmorillonite were completely exfoliated. The exfoliated platelets could then be extracted with two-phase toluene/NaOH to remove the organic exfoliating agents.

Exfoliated CNPs, usually in the form of an aqueous suspension, have been successfully introduced into various polymer networks to form nanocomposite hydrogels (Fig. 4). The typical approaches for this are *in situ* free radical polymerization, supramolecular assembly, and use of freezing–thawing cycles. For *in situ* free radical polymerization, the CNPs suspension can be added and mixed well with aqueous solutions of nonionic monomers such as acrylamide (AM)[51] or acrylamide derivatives, *e.g. N*,*N*-dimethylacrylamide (DMA) and *N*-isopropylacrylamide (NIPAM).[52] Moreover, in the polymerization of ionic monomers, such as acrylic acid (AA),[53] sodium methacrylate (SMA),[54] sodium 4-styrene sulfonate (SSNa) or 2-acrylamido-2-methylpropane sulfonic acid (AMPS), the charged CNPs were pre-adsorbed onto the monomers to avoid the aggregation of exfoliated CNPs. Well-exfoliated CNPs can also be introduced into pre-prepared polymeric hydrogel networks of poly(ethylene glycol) (PEG),[55] sodium polyacrylate (PAAS)[56]or poly(*N*-vinyl-2-pyrrolidone) (PVP)[57] to form hydrogels. In addition, exfoliated clay minerals can be mixed with pre-designed macromolecules in water to obtain clay mineral-containing nanocomposite hydrogels by supramolecular assembly.[58] Moreover, the mixture of exfoliated clay minerals or organically modified clay minerals and hydrophilic polymers (*e.g.*, poly(vinyl alcohol), PVA) and oligomers (*e.g.*, poly(ethylene glycol)diacrylate, PEGDA) can form clay mineral-containing nanocomposite hydrogels by treatment involving freezing–thawing cycles.[59,60]

2.2 *In situ* free radical polymerization

In situ polymerization is one of the most common methods for preparing nanocomposite hydrogels because the type of nanofillers and polymer precursors can be varied in a wide range to achieve desired properties (Table 1). In *in situ* free radical

Table 1 Clay mineral–polymer nanocomposite hydrogels synthesized by *in situ* free radical polymerization

Monomer	Clay mineral	Additives	Conditions	Properties	Ref.
AM	LAPONITE® RD; LAPONITE® RDS	TEMED; KPS: 20 mg mL^{-1}	30 °C 72 h	Elongation: >4000%; Strength: 110 kPa; relaxation modulus: ~0.16	51
AM: 3 g	LAPONITE® XLS: 0.5–2 g	TEMED: 24 μL; KPS: 20 mg mL^{-1}	30 °C 48 h	Adsorption of CV dye increased with increasing LAPONITE® concentration	68
NIPAM: 0.03 g	LAPONITE® XLG: 0.198–1.782 g	TEMED: 24 μL; KPS: 20 mg mL^{-1}	20 °C 20 h	Elongation: ~1000%; swelling/deswelling; transparency	69
SSNa: 5.00 g; AAG: 5.00 g	APTMA–MMT	APS	70 °C 4 h	Thermal stability: up to 400 °C; absorbability	70
AA: 7.20 g	CTAB–illite/smectite: 0.235 g	APS: 0.10 g; styrene: 0.15 g; NMBA: 0.0216 g; sodium alginate: 1.20 g	70 °C 3 h	Absorbability of methylene blue: 1843.46 mg g^{-1}	71
AMPS: 30.0 g	Chitosan: 1.0 g–MMT:4.0 g	APS: 0.15 g; PEGDMA: 0.24 g	70 °C	Absorbability: 440 g g^{-1}; thermal stability: up to 434 °C glass transition temperature: ~98.2 °C; elastic modulus: 238%	72 and 73
AA: 5–13 g	ODA–MMT: 0.30–1.10 g	Span 60: 0.3 g; BP: 0.03–0.05 g; NMBA: <0.01 g	70 °C 3 h	Absorbability in distilled water: 800 g g^{-1}; absorbability in saline solutions: $M^{+} > M^{2+} > M^{3+}$ decomposition with increasing temperature	67
AM	Bentonite	NMBA; APS	Sonication assisted	Swelling/deswelling	74
AM: 3 g	Halloysite: 6 g	KPS: 3 mL	65 °C 18 h	Swelling ratio: 4000%	75
Acryloyl chloride	LAPONITE® XLS	PEG; Irgacure 2959	UV irradiation λ = 365 nm, 45 mW cm^{-2}; 5 min	Compressive modulus: 48.6 kPa; fracture stress: 3882.8 kPa; toughness: 268.3 kPa	60

AA: acrylic acid; AM: acrylamide; AMPS: 2-acrylamido-2-methylpropane sulfonic acid; AAG: acrylamide glycolic acid; NIPAM: *N*-isopropylacrylamide; SSNa: sodium 4-styrene sulfonate; PEG: poly(ethylene glycol); PEGDMA: poly(ethylene glycol)dimethacrylate; APS: ammonium persulfate, BP: benzoyl peroxide used as initiator, and KPS: potassium persulfate as an initiator; APTMA: (3-acrylamidopropyl)trimethylammonium, CTAB: cetyltrimethylammonium bromide and ODA: octadecylamine as an organic modifier; MMT: montmorillonite; NMBA: *N*,*N*-methylene-(bis)-acrylamide as a cross-linker; TEMED: *N*,*N*,*N*′,*N*′-tetramethylene diamine used as a catalyst/accelerator; TSPP: tetrasodium diphosphate decahydrate used as a dispersing agent; CV: crystal violet.

polymerization, exfoliated CNPs are pre-prepared and mixed with an aqueous monomer solution to obtain a homogeneous dispersion of CNPs throughout the polymer matrix. The polymerization reaction is then initiated by external stimuli, such as thermal, photochemical, or chemical activation, through initiators and/or catalysts, which proceeds *in situ* on the surface of the CNPs (Table 1, Fig. 5a). Under such circumstances, both a chemically cross-linked polymeric network and physical entanglement of the polymer chains can be formed with CNPs distributed inside the network.[61] In other words, in the network, covalent interactions occur between neighboring polymeric molecules. It is also possible to form covalent bonds between the surface hydroxyl groups of the CNPs and polymeric molecules. Moreover, non-covalent interactions, including hydrogen bonding, electrostatic interactions, coordination bonds and hydrophobic interaction, namely, physical cross-linking, could exist in these nanocomposite hydrogels.[62,63] However, the quantification of these chemical and physical interactions remains difficult.

As summarized in Table 1, *in situ* polymerization is often initiated by chemical initiators,[64] such as ammonium persulfate, potassium persulfate, or benzoyl peroxide (BP), depending on the reaction. For example, Okay *et al.*[65] used ammonium persulfate as a redox initiator for the polymerization of AM in the presence of LAPONITE® CNPs, and produced polyacrylamide (PAM)/LAPONITE® nanocomposite hydrogels. Shen *et al.*[66] used potassium persulfate (KPS) as an initiator for polymerizing AA and obtained poly(acrylic acid (PAA)/LAPONITE® nanocomposite hydrogels. In these hydrogels, in addition to intermolecular interactions between the polymeric chains, LAPONITE® NPs served as cross-linkers between the PAA chains. Such additional interactions contributed by the CNPs become more complicated in the case of copolymerization. For example, a small amount of BP was used as an initiator in the preparation of nanocomposite hydrogels by grafting linear low density polyethylene (LLDPE) onto AA to form LLDPE-*g*-PAA/montmorillonite superabsorbent hydrogels.[67] In such a network, interactions between the –COOH or $–COO^-$ groups of AA and the –OH groups of the montmorillonite NPs are conceivable. Montmorillonite NPs specifically are utilized as multifunctional cross-linkers. As a result, a more stable and homogeneous hydrogel network can be achieved relative to single chemically cross-linked polymeric hydrogels without CNPs as cross-linkers.

Apart from polymerization initiated by chemical initiators, in the presence of a photoinitiator, polymerization can be initiated and facilitated by taking advantage of radiation (*via* electron beam or γ photons). As such, *in situ* polymerization in the solution of mixed CNPs and monomers can be conducted at mild or room temperature.[76] In addition, photopolymerization initiated using ultraviolet light or visible light is faster than polymerization using photochemical initiators.[60] Moreover, photoinitiated free radical polymerization offers an advantage of solvent-free formulation over thermally initiated free radical polymerization. For instance, using 1-hydroxy-cyclohexyl-phenylketone (Irg. 184) as the photoinitiator, Haraguchi *et al.*[77] prepared PNIPAM/LAPONITE® nanocomposite hydrogels by free radical polymerization under 365 nm UV light for 3 min. This method provided an efficient way of producing hydrogels in which uniformly dispersed LAPONITE® NPs acted as multifunctional cross-linkers, similar to that in polymerization initiated by chemical initiators. It is worth pointing out that CNPs can be modified with a photoinitiator beforehand, and the resultant hybrid can initiate the photopolymerization and provide CNPs *in situ* for the resultant polymeric networks.[78]

2.3 Supramolecular assembly

The direct mixing of macromolecules with clay minerals in water is a new facile route to produce nanocomposite hydrogels. Nevertheless, the macromolecules require functional groups that can directly cross-link with nano-sized clay mineral platelets in water. As demonstrated by pioneering study by Wang *et al.*,[58] a supramolecular nanocomposite hydrogel is obtained by directly mixing well-designed dendritic macromolecules with LAPONITE® NPs (Fig. 5b). The interactions between functional groups on the peripheries of the dendritic macromolecules and on the surface of the CNPs led to a novel supramolecular assembly. Thus, a high-water-content moldable hydrogel can be achieved. Interestingly, in this process, mixing water and LAPONITE® (2–3 wt%) with a very small proportion (<0.4 wt%) of organic components produced a transparent hydrogel. No catalysts or initiators were required for this assembly compared with the *in situ* free radical polymerization. Nonetheless, exfoliation of clay minerals and homogeneous dispersion of CNPs in water and on the surface functional groups of the macromolecules are two critical factors. Thus, the LAPONITE® can be effectively dispersed with the pre-treated sodium polyacrylate.

In addition, the dendritic structure of the macromolecules is critical for the formation of a supramolecular hydrogel network with dispersed CNPs in it. It was proved that the multiple guanidinium ion pendants of dendritic macromolecules are connected with oxyanions on the surface of CNPs through a salt-bridge formed by electrostatic interaction. Though the nanocomposite hydrogel was formed merely by non-covalent forces resulting from the specific design of a telechelic dendritic macromolecule with multiple adhesive termini for binding to clay, it showed a high mechanical strength, and rapidly and completely self-healed when damaged, and consequently it could be molded into shape-persistent, free-standing objects. Based on such methodology, well-designed linear macromolecules with proper surface functional groups can also cross-link with CNPs through a salt-bridge to form nanocomposite hydrogels. For example, Tamesue *et al.*[79] mixed a linear macromolecule with LAPONITE® XLG NPs, which were pre-dispersed in water with a minute amount of sodium polyacrylate. In this way, a supramolecular nanocomposite hydrogel composed of linear macromolecule and LAPONITE® XLG NPs was successfully obtained. Similarly, it was believed that the salt-bridge between the guanidinium ion on the terminal of the linear macromolecule and the oxyanions on the surface of the LAPONITE® NPs mainly contributed to the formation of a hydrogel with such a well-defined cohesive structure.

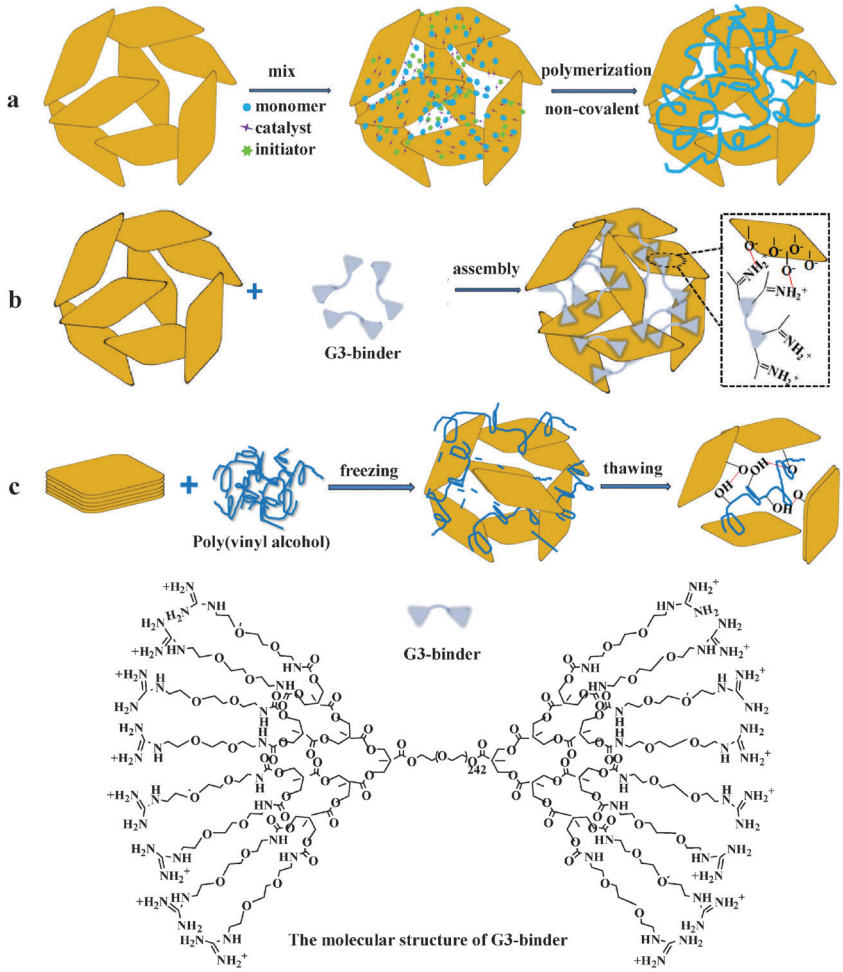

Fig. 5 Three methods to prepare clay-containing nanocomposite hydrogels: (a) *in situ* free radical polymerization usually starting from the mixture of a monomer, catalyst, and initiator under room temperature; (b) supramolecular assembly through the direct mixing of clay minerals with a pre-designed dendritic macromolecule, *i.e.* G3-binder, which carries adhesive dendron units at both termini of a long, hydrophilic polyethylene glycol (PEG) spacer. Adapted and reprinted by permission from Macmillan Publishers Ltd: [*Nature*] (ref. 58), copyright (2010); and (c) freezing–thawing cycles, starting from a mixture of poly(vinyl alcohol) (PVA) and clay minerals.

In comparison, linear macromolecules are less expensive than dendritic macromolecules. It is noteworthy that at sufficiently high concentrations and under electrostatic screening conditions, charged supramolecular polymers can easily produce a three-dimensional (3D) network that takes the form of a hydrogel. Therefore, it is possible that such a method could be applied to many other molecules with CNPs. In particular, a recent study revealed that small organic molecules can also form a supramolecular hydrogel through such supramolecular assembly and micro-crystallization.[80] However, whether the assembly to form small organic molecule-based hydrogels works in the presence of CNPs is still relatively unknown.

2.4 Freezing–thawing cycles

In addition to polymerization and supramolecular assembly, a physical cross-linking method can also result in the formation of an entangled, cross-linked hydrogel network.[81] It has been found that a freezing–thawing process of a mixture of polymer with clay minerals in water can facilitate the incorporation of clay minerals into the polymer networks. PVA is particularly suitable for use with clay minerals to form physically cross-linked hydrogels using freezing–thawing cycles.[82,83]

In this method, typically, PVA and montmorillonite are mixed in distilled water and heated to achieve complete dissolution.[84] Then, the aqueous solution consisting of clay minerals and polymers undergoes a freezing process, normally at −20 °C, with a subsequent thawing at room temperature in air. Repeating such a freezing–thawing operation results in the formation of a nanocomposite hydrogel with dispersed CNPs in it (Fig. 5c). The presence of clay minerals in the three-dimensional network of a hydrogel causes an increase in the cross-linking density, thus creating a more entangled structure.[84] Ibrahim and El-Naggar[85] also found that freezing–thawing cycles facilitated the entanglement of PVA chains, and further proved that the freezing–thawing cycles can drive cross-linking through hydrogen bonds between the hydroxyl group of the PVA chains and oxyanions on the surface of montmorillonite. Thus, physically cross-linked hydrogels with the ability to

undergo sol–gel transition can exhibit thermo-reversible performance. In addition, the resultant hydrogels can exhibit high thermal stability by increasing the clay content in the hydrogels. It is worth noting that in the freezing and thawing process, there is no need for any additional chemical or elevated temperature. Interestingly, the freezing and thawing techniques can be employed with electron beam (EB) irradiation to produce a PVA/clay hydrogel.[85]

3. Effects of clay minerals on the properties of nanocomposite hydrogels

The mechanical and thermal properties of the nanocomposites can be significantly enhanced when nano-sized platelets of clay minerals are uniformly dispersed in the polymer matrix.[86] Similar enhancements are also achieved when such clay minerals are incorporated into polymeric hydrogels. The exceptional toughness obtained through adding clay minerals in nanocomposite hydrogels[32] is attracting increasing research interest for this material over the last decade. In addition, loading CNPs into polymeric hydrogels can alter their optical transparency and anisotropy, as well as their swelling–deswelling and stimuli-responsiveness. Superficially, the effects of clay minerals on the properties of nanocomposite hydrogels are dependent on (1) the type of clay minerals (*e.g.*, the 1 : 1 type and the 2 : 1 type); (2) the concentration of CNPs in the network; and (3) the dispersion degree of CNPs in the network structure. However, the physical and chemical interactions between polymers and CNPs are of paramount importance.[87,88]

3.1 Optical properties

Hydrogels with high optical transparency are paving the way for many new innovations such as transparent wound dressing with optical clarity for facile wound inspection[89] and sensors with an optical response (transparency and optical anisotropy) that can vary with an external stimulus such as a temperature change.[90,91] The addition of clay minerals into polymeric hydrogels can be used to tune the optical transparency of the nanocomposite hydrogels. The optical transparency is related to the uniform structure in the nanocomposite hydrogels.[92] Remarkably, PNIPAM/LAPONITE® nanocomposite hydrogels have a high transparency regardless of the concentration of LAPONITE® in the concentration range of 1×10^{-2}– 25×10^{-2} mol L^{-1}.[93] When the concentration of LAPONITE® is less than 10×10^{-2} mol L^{-1}, the PNIPAM nanocomposite hydrogels show a sharp decrease in transparency at the lower critical solution temperature (LCST).[94] When the concentration of LAPONITE® is more than 10×10^{-2} mol L^{-1}, the transparency remains constant regardless of the LCST because the thermal-molecular motion of the polymers is completely restricted by exfoliated LAPONITE® nanoplatelets in the network of the nanocomposite hydrogels.

CNPs can also affect the ordering and the crystallization behavior of polymers, leading to changes in the optical anisotropy.

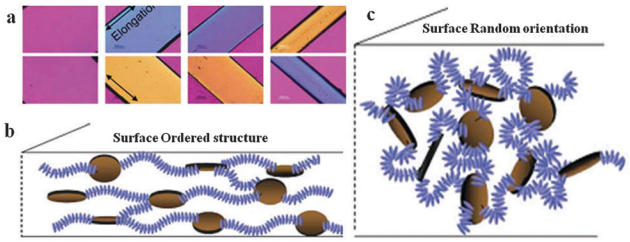

Fig. 6 (a) Polarized-light micrographs (left to right) of stretched nanocomposite hydrogels consisting of poly(*N*-isopropylacrylamide) PNIPAM and LAPONITE® XLG at a strain of 0%, 300%, 740% and 1300%, respectively. The tests were conducted under crossed polarizers in conjunction with a 530 nm retardation plate, where +45° (−45°) orientation is parallel to the slow (fast) axis of the retardation plate. (b) The stretched state of the nanocomposite hydrogels. (c) The unstretched state of the nanocomposite hydrogels. PNIPAM chains and clay platelets are randomly oriented in the nanocomposite hydrogels that are non-birefringent. Adapted and reprinted from ref. 95 with permission of The Royal Society of Chemistry.

Murata and Haraguchi[95] revealed that for nanocomposite hydrogels with PNIPAM/LAPONITE® XLG network structures, the optical anisotropy exhibited unique changes when the nanocomposite hydrogels were deformed uniaxially. The optical anisotropy of clay mineral-containing nanocomposite hydrogels can be measured by the birefringence phenomena. Herein, the birefringence phenomena of nanocomposite hydrogels correlate with the orientation of polymers and CNPs in the network structure,[95] where the distinct maxima and sign inversions are indicative of strain and the hydrogel composition (Fig. 6a). Such PNIPAM/LAPONITE® XLG nanocomposite hydrogels present an ordered structure on uniaxial stretching (Fig. 6b) and exhibit strong birefringence due to the optical anisotropy.[96] In the unstretched, isotropic state (Fig. 6c), however, PNIPAM chains and CNPs are randomly oriented in the nanocomposite hydrogels, resulting in non-birefringence. In addition to the polymer chains, the alignment of CNPs in aqueous colloidal dispersions is subjected to an external force, which thereby induces a structural ordering together with separation and distribution of CNPs.

3.2 Mechanical properties

The mechanical properties of pure polymeric hydrogels are typically weaker than hydrogels with reinforcement nanoparticles, where inorganic fillers can offer additional adhesion with a polymer matrix. In contrast to 1D or 3D nanoparticles, negatively charged lamellar clay nanosheets embedded within polymeric networks enable the hydrogels to exhibit more exceptional mechanical properties. Earlier, Haraguchi *et al.*[34] investigated PNIPAM/LAPONITE® nanocomposite hydrogels with the concentration of LAPONITE® up to 25×10^{-2} mol L^{-1} H_2O. The resultant hydrogels exhibited remarkable increases in tensile strength (1.1 MPa) and modulus (453 kPa). These clay mineral-containing nanocomposite hydrogels interestingly can be elongated to more than 1000% of their original length.[97] The enhanced tensile behavior of clay-containing nanocomposite

hydrogels is attributed to their unique network of uniform cross-linking between the CNPs and the long, flexible polymer chains. In particular, the homogeneous dispersion of clay nanoplatelets into the polymer network at a nanometer scale can assist in obtaining a narrow length distribution of polymer chains, and can subsequently result in a superior tensile behavior of the nanocomposite hydrogels.

The increased tensile strength and modulus are attributed to the additional physical and/or chemical interactions among the polymers, colloidal CNPs, and water. Chang *et al.*[60] prepared PEGDA/LAPONITE® nanocomposite hydrogels with enhanced mechanical properties by harnessing the ability of PEGDA oligomers to simultaneously form chemically cross-linked networks while binding with LAPONITE® nanoparticles through secondary interactions.

The significant enhancement of the compressive and tensile properties of the PEGDA hydrogels was primarily ascribed to the incorporation of LAPONITE® nanoparticles, and was affected by the molecular weight of PEG and the concentration of the LAPONITE® nanoplatelets. Thus, the synergistic interactions become more complicated because of the presence of CNPs in the polymeric networks, which play a key role in the mechanical behavior of the nanocomposite hydrogels.[98] At present, the inherent reasons for the exceptional toughness of clay nanocomposite hydrogels remain elusive and require further investigation. In addition, clay minerals can improve the hydrophilicity and flexibility of networks, resulting in increases in tensile strength and modulus.[99]

Similarly, the compressive strength and modulus increase almost proportionally to the concentration of clay minerals, but such a conclusion is simply applicable to the cases in which a specific type of CNP and its amount in a certain range is used (*e.g.*, for LAPONITE®, lower than 25×10^{-2} mol L^{-1}).[100,101] In the case of the addition of LAPONITE® CNPs, at concentrations below 10×10^{-2} mol L^{-1} H_2O, a recovery of 90–99% from elongation of 900% was achieved. When the concentration was higher than 10×10^{-2} mol L^{-1} H_2O, the recovery decreased significantly with the increasing concentration of LAPONITE®.[102] Considering that CNPs are a class of negatively charged lamellar nanoplatelets, a recent breakthrough on nanocomposite hydrogels using negatively charged unilamellar titanate nanosheets is worth discussing.[103] It was found that a strong magnetic field can induce co-facial nanosheet alignment in aqueous colloidal dispersions, which can maximize electrostatic repulsion, and thereby induce a quasi-crystalline structural ordering over the macroscale, along with a uniformly large face-to-face nanosheet separation. This transiently induced structural order can be tactically fixed by transforming the dispersion into a hydrogel using light-triggered *in situ* vinyl polymerization. The resultant hydrogel containing charged inorganic structures can align co-facially in a magnetic flux and deform easily under shear forces applied parallel to the embedded nanosheets, yet it can resist compressive forces applied orthogonally. These findings clearly reveal that soft materials using 2D nanoparticles can lead to unique functions.

3.3 Swellability

Swellability and delamination are characteristic of clay minerals such as montmorillonite, hectorite and synthetic LAPONITE®. These properties are comparable with the swellability of certain polymeric hydrogels. Nanocomposite hydrogels consisting of water-swellable clay minerals, *e.g.*, LAPONITE® or montmorillonite, exhibit peculiar swellability, including a high swelling rate, a large but finite equilibrium swelling ratio and spontaneous deswelling in water.[104,105] For example, Zhang *et al.*[106] reported that a PAA/montmorillonite nanocomposite hydrogel showed a higher swelling ratio than their corresponding clay-free hydrogels. It was suggested that montmorillonite NPs helped to form a highly loose and porous structure in the nanocomposite hydrogels, and thereby improved the swelling ratio of the PAA/montmorillonite nanocomposite hydrogels.[107] First, the polymer chains in the unique network structure were more flexible for swelling when physically cross-linked by CNPs, as opposed to the situation in a pure chemically cross-linked polymer network. Second, the increment of swellability was attributed to the increased ionic osmotic pressure resulting from the mobile ions on the surface of clay minerals and the hydrated cations in the interlayer. Due to the negative charge on the surface of CNPs, sodium counterions were uniformly dispersed in the network of hydrogels. The hydrogels consequently swelled in pure water, allowing water molecules to enter into the network and diffusion of mobile sodium ions from the network until an equilibrium swelling state was reached (Fig. 7). The swelling state was dependent upon the release of sodium ions, and the deswelling of the nanocomposite hydrogels appeared spontaneously. This swelling–deswelling behavior is also apparent in the network structure of nanocomposite hydrogels consisting of nonionic polymer PAM and LAPONITE® RD.[108] It has been observed that with swelling a substantial volume of water is entrapped within

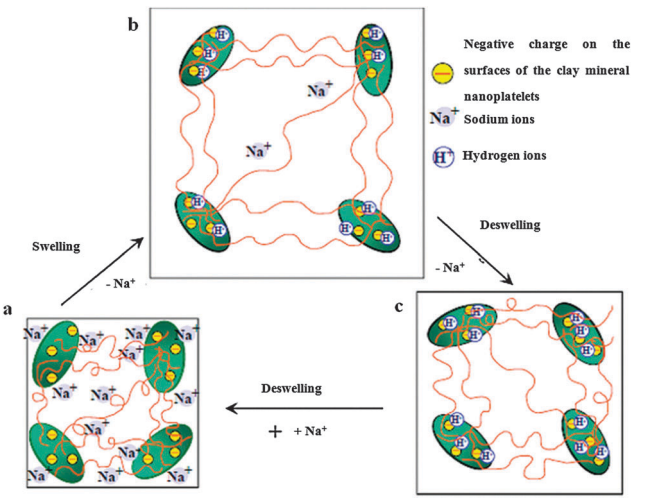

Fig. 7 The swelling–deswelling behavior in the network structure of nanocomposite hydrogels consisting of non-ionic polymer poly(*N*,*N*-dimethylacrylamide) (PDMA) and LAPONITE® XLG: (a) as-prepared state; (b) maximum swelling state; and (c) equilibrium swelling state. Only a few polymer chains and counterions are depicted for simplicity. Adapted with permission from ref. 105. Copyright (2011) American Chemical Society.

the hydrogels because of osmotic pressure changes and the movement of free ions between the hydrogels and solution. The hydrogels can swell to an equilibrium state, during which the outflow of mobile ions leads to a low ionic osmotic pressure and, subsequently, to deswelling. It is noteworthy that such an increment is also caused by the CNPs used in the hydrogels. For instance, Darvishi *et al.*[109] obtained a maximum swelling ratio for poly(AMPS-*co*-*N*-[3-(dimethylamino)propyl]methacrylamide (DMAPMA))/bentonite anionic–cationic nanocomposite hydrogels with 10.2 wt% of nanobentonite. Kaşgöz *et al.*[110] drew a similar conclusion for poly(2-acrylamido-2-methylpropane sulfonic acid) (PAMPSA)/LAPONITE® nanocomposite hydrogels, where LAPONITE® in a fraction greater than 10 wt% in the hydrogels resulted in a lower swelling ratio. For instance, with a content of 10 wt% LAPONITE®, the nanocomposite hydrogels reached the maximum swelling ratio (164.3 g water per g sample). The increase in the concentration of CNPs led to a higher cross-linking density in the network structure.[111,112] By further increasing the concentration of CNPs, there was a reduction in the swelling ratio, owing to the higher cross-linking density in the network structure, which thus could not be expanded so easily.[113]

Similar phenomena were observed when LAPONITE® was utilized for PNIPAM/LAPONITE® nanocomposite hydrogels,[114] and when attapulgite was used for PAA/attapulgite nanocomposite hydrogels.[115] In comparison to attapulgite, kaolinite, and mica, PAM/Na^+-montmorillonite nanocomposite hydrogels exhibit a higher swelling rate in distilled water.[116] Zhang and coworkers[116] compared the effects of different types of clay minerals with a concentration of 10 wt% of montmorillonite, attapulgite, and kaolinite on the swelling behaviors of PAA-based hydrogels in a cationic saline solution.[117] The PAM/attapulgite nanocomposite hydrogels showed the highest swelling ratio in NaCl solution, while in $FeCl_3$ solution, the PAM/kaolinite nanocomposite hydrogels exhibited the highest swelling ratio.

3.4 Stimuli-responsiveness

The stimuli-responsiveness of nanocomposite hydrogels refers to the phenomena of their volume and transparency changing reversibly in response to the surrounding stimuli, such as temperature, pH, ionic strength, pressure or electronic field.[118,119] Such properties are of great importance in smart optical materials, diagnostics, biosensors, drug delivery, tissue engineering, coatings and micro-electromechanical systems.

For a given nanocomposite hydrogel, chemically cross-linked networks have permanent connections, while physical networks have transient junctions that arise from either polymer chain entanglements or physical interactions. The use of added CNPs varies the chemically cross-linked networks and physical networks. As a result, CNPs can be used to tune the stimuli-responsive behaviors of nanocomposite hydrogels in terms of their volume and transparency.[120] The stimuli-responsiveness of clay mineral-containing nanocomposite hydrogels results from the changes in conformation, ordering, or solubility of the constituent polymers and CNPs. For example, physically cross-linked clay mineral-containing nanocomposite hydrogels can undergo a SGPT. Typically, a clay mineral-containing nanocomposite hydrogel formed *in situ* by reversible physical networks can readily present reversible sol–gel phase transitions induced by external stimuli. The changes can mainly be attributed to the interactions among the polymer chains, CNPs and water, such as hydrophobic interaction, electrostatic interaction and hydrogen bonding. Chemically covalently cross-linked, clay mineral-containing nanocomposite hydrogels basically have permanent networks, which can undergo VPT and changes of optical properties.

On the one hand, CNPs contain hydrophilic edges with cations in the interlayer space and a hydrophobic silanol surface. Thus, the addition of clay minerals in the polymeric networks can modify the hydrophilic–hydrophobic balance of the polymers. As thermo-responsiveness is strictly regulated by the balance of hydrophilic and hydrophobic forces in the network structure, the addition of CNPs affects the thermo-responsiveness of the nanocomposite hydrogels.[121] Typically, thermo-responsive PNIPAM includes both hydrophilic (–CONH–) and hydrophobic ($-CH(CH_3)_2$) groups.[122] PNIPAM chains show a thermally triggered conformational change from a hydrophilic coil to a hydrophobic globular form at LCST (about 32 °C). The addition of clay minerals can change the conformation of the network structure of the nanocomposite hydrogels, thereby tuning the stimuli-responsiveness. In particular, the thermally triggered conformational change of polymer chains in clay mineral-containing nanocomposite hydrogels is significantly restricted by clay minerals because of interactions between the PNIPAM chains and clay minerals through hydrogen bonding. The PNIPAM chains in nanocomposite hydrogels exhibit a coil-to-globule transition at higher temperatures than for normal PNIPAM chains,[123] indicating that there is a thermodynamic balance between hydrophilic and hydrophobic interactions in aqueous media.[124]

On the other hand, clay mineral-containing nanocomposite hydrogels can exhibit a better pH-responsiveness in comparison to single-polymer hydrogels, because conventional hydrogels are cross-linked by small molecules and always show a slower response rate and inferior elasticity.[125] The pH-responsiveness of hydrogels is usually attributed to their ionic groups. In particular, montmorillonite[126] and LAPONITE®[127] are more or less pH-dependent due to the edge charges. The addition of these clay minerals can increase the ionization of polymers, following a chain expansion in response to pH. Recently, Li *et al.*[128] successfully synthesized pH/temperature double-responsive nanocomposite hydrogels consisting of poly(DMA-*co*-(2-dimethylamino)ethyl methacrylate (DMAEMA)) cross-linked by LAPONITE® NPs. In addition, due to the extra ionic charge provided by CNPs, the incorporation of CNPs into the polymer hydrogels brought about distinct nanocomposite hydrogels that can undergo significant electro-responsive changes.[129] The ion concentration on the surface of the CNPs can accelerate the electro-responsive rate, whereas the cross-linking density of the network in the hydrogels can impede the electro-responsive rate. Such nanocomposite hydrogels containing charged inorganic CNPs may undergo exceptional changes either in mechanical or

optical behavior in response to the alternating application and removal of an electric field, with these changes arising from the varied alignment of CNPs and the polymeric chains.[130]

4. High functional applications of clay mineral-containing nanocomposite hydrogels

4.1 Superabsorbents

A high water uptake is a key characteristic of polymer hydrogels.[131] Clay minerals also have a remarkable adsorption capacity for water and many other inorganic and organic cations. The combination of these two components leads to nanocomposite hydrogels with a very distinct adsorptive behavior. In many cases, smectite clay mineral-containing nanocomposite hydrogels have higher adsorption capacities, a faster adsorption rate, and enhanced mechanical stability than polymeric hydrogels.[108,113] Moreover, smectite clay minerals have abundant exchangeable cations in the interlayer space and negative charges on their surface. These performances of clay minerals make their nanocomposite hydrogels effective as superabsorbents to remove heavy and toxic metal ions[132] and cationic dyes[133] from sewage water.

The presence of clay minerals as cation exchangers enables clay mineral-containing nanocomposite hydrogels to possess active sites to adsorb heavy metal ions.[134] The adsorption mainly results from the strong electrostatic interactions between the smectites and metal ions.[135] In addition, some heavy metal ions can be absorbed by clay mineral-containing nanocomposite hydrogels through coordination bonds, hydrogen bonds, or/and by dipole association. For example, a study by Güçlü *et al.*[136] suggested that PAA/montmorillonite nanocomposite hydrogels can be used for the removal of copper(II) and lead(II) ions from water. In this study, the adsorption reached equilibrium within 24 h at pH = 4 and room temperature. Ibrahim and El-Naggar[85] prepared PVA/clay nanocomposite hydrogels through freezing and thawing, followed by electron beam irradiation for the treatment of wastewater, and revealed that the PVA-based hydrogels consisting of 60% of montmorillonite used as fillers exhibited a higher adsorption capacity for ions such as Cu^{2+}, Ni^{2+} and Co^{2+} from wastewater.

In addition to the removal of inorganic heavy metal ions, clay mineral-containing nanocomposite hydrogels can also be used to remove cationic dyes from wastewater. The adsorption of nanocomposite hydrogels for cationic dyes can be attributed to the electrostatic interaction between anions on the surface of the clay minerals and the active groups of the dyes (Fig. 8). Li *et al.*[68] prepared PAA/LAPONITE® nanocomposite hydrogels as superabsorbent materials for adsorbing monovalent cationic dyes. The dye adsorption rate and equilibrium amount increased significantly with the increased concentration of clay minerals up to 20 wt% in hydrogels. Mahdavinia *et al.*[137] found that the adsorption capacity of nanocomposite hydrogels composed of kappa-carrageenan, sodium alginate and sodium montmorillonite for cationic crystal violet dyes was approximately 2–6 times

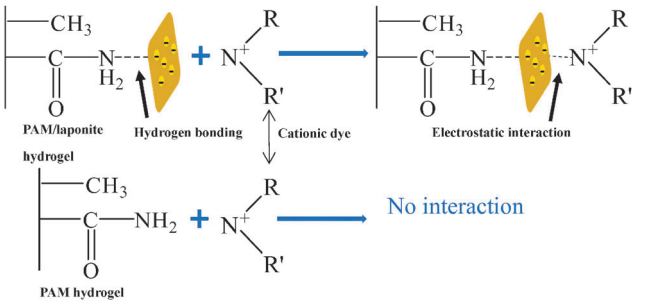

Fig. 8 The mechanism of cationic dye adsorption by clay mineral-containing nanocomposite hydrogels. The negative charges on the surface of the clay mineral (LAPONITE®) in nanocomposite hydrogels can readily interact with cationic dye molecules through electrostatic interaction, while poly(acrylamide) (PAM) hydrogels without clay minerals could not interact with the dyes. Ref. 68. Copyright (©) [2008] [John Wiley and Sons].

higher than that of hydrogels consisting of alginate alone. The adsorption rate of the dyes onto alginate nanocomposite hydrogels also increased due to the addition of the charged montmorillonite. Moreover, the negatively charged surface of clay minerals can be modified by grafting with a variety of functional groups. For example, the surface of CNPs was covalently functionalized with aminopropyl groups to yield aminoclay (AC) (Fig. 9a). AC with aminopropyl groups on the surface was then assembled to form functional hydrogels. Accordingly, the resultant hydrogels were able to absorb anionic dyes such as coronene tetracarboxylate salt and perylene tetracarboxylate salt (Fig. 9b). The increase in the adsorption capacity and adsorption rate of dyes onto superabsorbents are affected by both the swellability and porosity, resulting from the addition of such clay minerals. For most dyes, the adsorption onto nanocomposite hydrogels

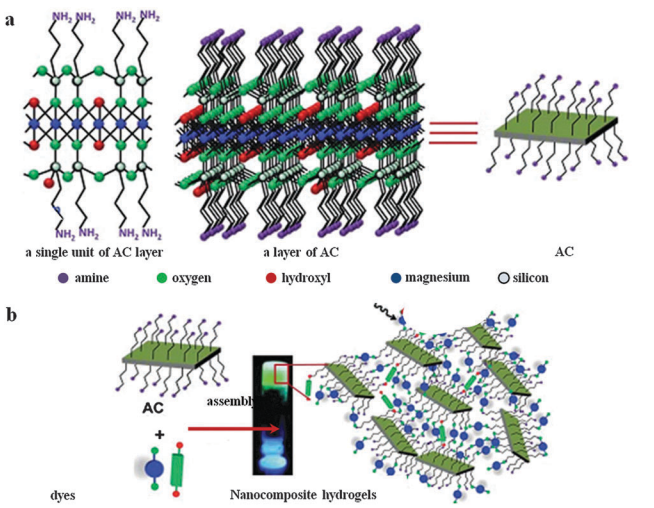

Fig. 9 (a) Schematic representation of a single unit and a layer of aminoclay (AC), which was covalently functionalized with aminopropyl groups. (b) AC with aminopropyl groups on their surface formed hydrogels, and the hydrogels were then used to absorb different anionic dyes: coronene tetracarboxylate salt (blue) and perylene tetracarboxylate salt (green). Adapted from ref. 139 with permission of The Royal Society of Chemistry.

correlates well with the Langmuir isotherm equation, and the adsorption kinetics onto the hydrogel composite is consistent with the pseudo-second-order model.[138]

4.2 Biomedical and pharmaceutical materials

4.2.1 Vehicles for drug delivery and controlled release. Polymeric hydrogels with an open network as drug vehicles normally undergo rapid drug release in an uncontrolled manner, causing drug distribution to various organs and compartments in the body indiscriminately.[140] Hydrogel structures with clay minerals have achieved the ability to tune drug release, in addition to improving the resistance of loaded drugs from degradation.[141,142] The cationic drug species are bound to the CNPs *via* adsorption on the negatively charged clay mineral surface.[143] The binding of drugs onto montmorillonite results from a cation exchange reaction between cationic drug ions and cations in the interlayer space of the clay minerals. In addition, a drug can also be attracted and loaded on to CNPs by surface adsorption. In contrast, neutral drugs can simply be bound through their interactions with active sites on the surface of the clay minerals in the hydrogels network.[144]

Depending on the drugs, CNPs and polymers, the interactions can be physical or chemical or both. Chemical adsorption is stronger than conventional physical adsorption. Importantly, in some nanocomposite hydrogels, clay minerals play a leading role in the adsorption of drugs.[145] For example, Anirudhan and Sandeep[146] studied nanocomposite hydrogels consisting of carboxymethyl chitosan and montmorillonite, and found that the negatively charged montmorillonite nanoplatelets encapsulated 94.56% of doxorubicin, a neutral drug, *via* hydrogen bonding and electrostatic interactions. The release of doxorubicin from the nanocomposite hydrogels was related to the breakage of the bonds and hydrogel dissolution. Moreover, the addition of montmorillonite shifted the dissolution-resistant properties of hydrogels, thereby affecting the release of drugs.[147] Kevadiya *et al.*[148] synthesized montmorillonite/alginate nanocomposite hydrogels with the intercalation of lidocaine hydrochloride (LC), an antiarrhythmic local anesthetic drug, into montmorillonite. Due to the host–guest intercalation and the pH-responsiveness of the alginate/montmorillonite nanocomposite hydrogels, LC was released from montmorillonite in the hydrogels in a controlled way. Kevadiya *et al.*[149] demonstrated that PAM/Na^+-montmorillonite nanocomposite hydrogels produced by free radical polymerization had the potential to be used as an anticancer drug carrier reservoir. The addition of the hydrophilic montmorillonite improved the water uptake of the nanocomposite hydrogels. An *in vitro* study of drug release showed that the release from the nanocomposite hydrogels was controlled with time and partial diffusion through the swollen matrix of the nanocomposite hydrogel.[149] As shown by the above-mentioned examples, recent progress indicates that clay mineral-containing nanocomposite hydrogels have excellent potential as drug carriers.

4.2.2 Scaffold for tissue engineering. CNPs can combine with the macromolecules, such as poly(NIPAM-*co*-DMAEMA)),[150] PEO,[151] PVA, PAA, polypeptides,[152] alginate and chitosan,[153] to form biocompatible nanocomposite hydrogels. Such hydrogels have been tested as scaffolds for organizing and directing cells to form a desired tissue, and thus the tissue can be delivered in a minimally invasive manner.[154] Many types of cells, for example, the osteoblast,[72] murine fibroblast,[155] stem cells,[156] epithelial cells, human hepatic cells, dermal fibroblasts, and umbilical vein endothelial cells,[157] have shown good adhesion, differentiation and proliferation on clay mineral-containing nanocomposite hydrogels *in vitro*.

The binding of the cell to the nanocomposite hydrogels surface is driven mainly by electrostatic interactions. For example, Kotobuki *et al.*[158] synthesized DMA nanocomposite hydrogels consisting of 2×10^{-2} mol L^{-1} of LAPONITE® for the cultivation, differentiation, and proliferation of human mesenchymal stem cells. Both the hydrophilic DMA and the charged LAPONITE® enhance the binding of cells to the nanocomposite hydrogels. Though PEG hydrogels are not an adhesive to cells, adding 5% of LAPONITE® as the cross-linker to form the PEG/LAPONITE® nanocomposite hydrogels can enable the materials to support cell adhesion.[102] Here, the LAPONITE® in the covalently cross-linked network was mainly responsible for the adhesion. Chang *et al.*[60] synthesized biocompatible PEGDA/LAPONITE® nanocomposite hydrogels that can support both two- and three-dimensional (2D and 3D) cell cultures. Unlike PEGDA hydrogels, PEGDA/LAPONITE® nanocomposite hydrogels supported cell adhesion and their subsequent spreading in a 2D culture, as well as supported 3D cell encapsulation similar to that of the widely used PEGDA hydrogel systems. Moreover, the addition of LAPONITE® wielded no adverse effect on the encapsulated cells. Similarly, by adding 20–70% of LAPONITE® NPs to PEO, Gaharwar *et al.*[159] prepared nanocomposite hydrogels with higher cell viability ($\sim$95%) than that on a PEO hydrogel. The presence of montmorillonite also enhanced the cellular uptake efficiency of carboxymethyl chitosan nanocomposite hydrogels through hydrogen bonding. The nanocomposite hydrogels maintained good cell viability even after 96 h.[146] Due to the addition of LAPONITE® XLG to poly(2-methoxyethyl acrylate) (PMEA)-based hydrogels, cells were successfully cultured on the surfaces of nanocomposite hydrogels.[160] The adhesion and proliferation of the cells increased with the increasing concentration of LAPONITE® in the range of 10–23 wt%. Clearly, CNP-containing nanocomposite hydrogels have enhanced mechanical properties and hence possess the potential to be used as scaffolds for tissue engineering. In addition, the ability of the nanocomposite hydrogels to support a 3D culture of encapsulated cells establishes them as an ideal injectable system with minimally invasive strategies for *in vivo* applications.

4.2.3 Biosensors. Clay mineral-based materials have long been considered as biosensors.[161] Combined with stimuli-responsiveness to the environment of the polymeric hydrogels, clay mineral-containing nanocomposite hydrogels as biosensors have additional advantages. Namely, the clay mineral-containing nanocomposite hydrogels consist of two basic components: (1) a recognition system and (2) a specific place for the sensitivity to occur. Earlier, by coating a silicon-integrated thermotransducer with a thin PAM/montmorillonite hydrogel membrane, containing time-dependent water vapor absorption, Gao *et al.*[162]

successfully constructed a sensor with high selectivity and high sorption capacity for liquid water and water vapor. Such a sensor showed an excellent reproducibility of the signal output voltage. A recent breakthrough by Ikeda *et al.*[163] featured a semi-wet fluorescent sensor by integrating supramolecular hydrogels with montmorillonite. Moreover, cationic coumarin dyes were intercalated into the interlayer space of montmorillonite for probing spermine and spermidine, as these can be used as biomarkers for assessing the effectiveness of cancer chemotherapy (Fig. 10). In this system, the organic supramolecular fibers formed the hydrogel and acted as an immobilization matrix, while the anionic montmorillonite NPs played a critical role in the interactions between the fluorescent molecules and biomarkers, where the montmorillonite NPs served as a host for the aggregation of the exchangeable cationic fluorescent dyes, and then such exchangeable cations could be replaced by polyamines through electrostatic interactions and this could be detected upon a color change. As a result, a color change occurs, which can be easily detected even with naked eyes in a user-friendly manner. Such a novel methodology provides a promising means for early cancer diagnosis in urine. This functional clay mineral-containing supramolecular hydrogel can also be taken as a model for designing sensor systems for a variety of analytes. In addition to montmorillonite, LAPONITE® has also been used as a host to provide space for transforming signals in the hydrogel biosensor.[164] Importantly, both the polymer and clay minerals can be further modified with functional groups to optimize the sensitivity and selectivity for targeted biomolecules.

4.2.4 Wound dressing. Wound dressings are often used to accelerate wound healing and create a moist environment. Moreover, an ideal wound dressing should be able to absorb the wound exudates and protect the wound from secondary infections.[165] The addition of clay minerals to the polymeric hydrogels and interactions with the polymers can improve the mechanical properties and absorptivity of nanocomposite hydrogels.[166] Clay mineral-containing nanocomposite hydrogels with suitable strength and elasticity can be expected to be an effective wound dressing material. Moreover, due to the enhancement of adsorption caused by the CNPs, the nanocomposite hydrogels can more efficiently absorb the wound exudates and keep the wound clean.[84] In addition, clay mineral-containing nanocomposite hydrogels with a large amount of water can keep the wound moist, and also protect the wound from infection.

Furthermore, CNPs in the hydrogels can tune the viscosity. Shen *et al.*[167] prepared PAA/LAPONITE® nanocomposite hydrogels showing adjustable viscosity by adjusting the amount of LAPONITE®. The increased viscosity is beneficial for wound dressing to tightly adhere into the wound. In particular, when organically modified CNPs are used, it is possible for the hydrophobic organo-CNPs to encapsulate organic drugs and control the release of the drugs. Using the freezing–thawing method, Kokabi *et al.*[84] prepared PVA/CTA^+-montmorillonite nanocomposite hydrogels (CTA^+: cetyltrimethylammonium cation) as wound dressings. The addition of CTA^+-montmorillonite plays a key role in nanocomposite hydrogels obtaining a relatively high adsorption capacity, appreciable vapor transmission rate, excellent barrier against microbe penetration, and excellent mechanical properties. The amount of the clay added to the nanocomposite hydrogel was found to be a key factor for the properties desired for wound dressing.

The *in vivo* evaluation of such PVA/organoclay nanocomposite hydrogels as an applicable wound dressing on animals also showed an improved healing process for wounds.[85] The improvement was attributed to the better creation of moist surfaces on the wound with less scar formation, a shorter duration of healing, and better closing of the wound edges with enhanced tensile properties of the healed wound, *i.e.*, increased tensile strength and elongation at break. In addition, an *in vitro* cytotoxic assay showed that the as-prepared nanocomposite hydrogel was non-toxic and biocompatible. In particular, when organically modified CNPs are used, it is possible for the hydrophobic organo-CNPs to encapsulate organic drugs, and then to control the release of the drugs. Importantly, in this way, organic drugs, which inherently cannot dissolve in water, can be introduced into the hydrogel using organo-CNPs as the intermediary. However, to date, this strategy has rarely been reported for clay mineral-containing nanocomposite hydrogels.

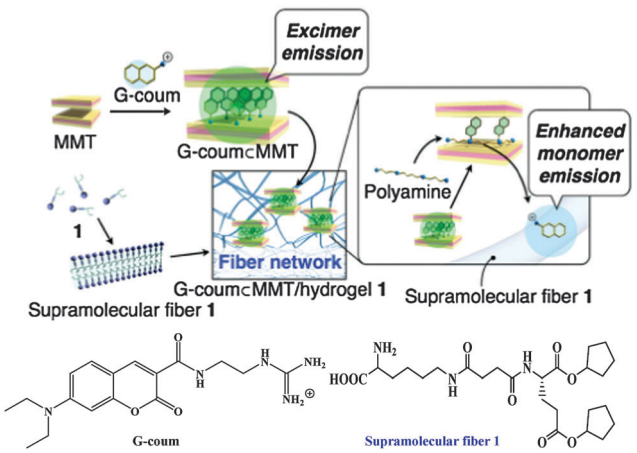

Fig. 10 Hybrid biosensor consisting of a cationic fluorescent coumarin dye (G-coum) intercalated into supramolecular fiber 1/montmorillonite (MMT) hydrogels for the determination of polyamines. The adsorbed cationic dyes in the interlayer space showed a weak greenish color, which converted to an intense blue color. Adapted and reprinted with permission from ref. 163. Copyright (2011) American Chemical Society.

5. Conclusions and outlook

Exfoliated clay minerals with a high aspect ratio are unique functional colloidal 2D nanoplatelets, which can be incorporated into hydrophilic polymers to form a novel class of nanocomposite hydrogels. The inorganic clay nanoplatelets physically and/or chemically interact with a polymer matrix, thereby causing a dramatic improvement in the mechanical properties, swellability, and adsorption of the resultant hydrogels. The stimuli-responsiveness of the nanocomposite hydrogels to temperature,

pH, and even an electric field can also be significantly tuned by adding clay minerals into the hydrogels. Clay mineral-containing hydrogels may thus serve as model systems to investigate the mechanisms behind the preparation and performance of many other two-dimensional inorganic nanosheets.

Substantial advances in such nanocomposite hydrogels have been achieved over the past few years. Nevertheless, to manufacture clay mineral-containing nanocomposite hydrogels in an effective way, and to endow the hydrogels with superior properties is still highly challenging.

(1) Due to the additional interfacial interactions in the nanocomposite hydrogels, the analysis of particular interactions and the mechanisms of the performance enhancements become more complicated and the fundamental reasons thus remain elusive. Thus, further studies are required to investigate the interactions that are intrinsic to these unique properties. Such a mechanistic understanding will provide in-depth insights into the structure–function relationships, which is critical for formulating controlled preparations for desired applications. As such, there is a need for the precise microstructural determination of interfacial and colloidal phenomena, *in situ* observation of the hydrogel formation, and linking at the molecular and atomic levels. To this end, computer simulation and theoretical calculations may also assist the theoretical modeling, prediction, and description of the structure and properties of clay mineral-containing nanocomposite hydrogels.

(2) *In situ* free radical polymerization is a common method to prepare nanocomposite hydrogels, because of its adaptability to various clay minerals and monomers. Currently, the rapid supramolecular assembly and the freezing–thawing process method are merely applicable to a few macromolecules or polymers. For these two methods, there is a large research space for rationally designing macromolecules or polymers with functional groups, such that the resultant hydrogel can meet the need for greater biocompatibility, faster response to stimuli, and increased mechanical properties. In addition, efficient exfoliation methods for clay minerals require further development, as uniformly-distributed CNPs in nanocomposite hydrogels are a key indicator of effectiveness for all preparation methods, and for the performance of the nanocomposite hydrogels.

(3) The applications of clay mineral-containing nanocomposite hydrogels cover a spectrum spanning from superabsorbents for wastewater treatment to biomaterials. In particular, clay mineral-containing nanocomposite hydrogels are attractive as vehicles for the controlled encapsulation and release of drugs, as tough and adjustable scaffolds for tissue engineering, as nanosized biosensors for diagnosis, and as wet and soft dressings for wound healing. Nevertheless, most studies are still conducted at a laboratory scale. The biological stability and the side effects of nanocomposite hydrogels require *in vivo* investigations. In addition, studies are rarely carried out on the use of the clay mineral-containing nanocomposite hydrogels in notch-sensitivity and self-healing ability, and as a cell-emulating system for photocatalysis.[80] Finally, more attention is required for combining the advantages of layered clay minerals and polymers, both of which can be modified and functionalized diversely. As such, there are many new possibilities that still remain for developing clay-containing hydrogel soft materials with unusual functions and wide applications.

Abbreviations

Polymers

LLDPE	Linear low density polyethylene
PAA	Poly(acrylic acid)
PAM	Polyacrylamide
PAMPSA	Poly(2-acrylamido-2-methylpropane sulfonic acid)
PDMA	Poly(*N*,*N*-dimethylacrylamide)
PEG	Poly(ethylene glycol)
PEGDA	Poly(ethylene glycol)diacrylate
PEGDMA	Poly(ethylene glycol)dimethacrylate
PEO	Polyethylene oxide
PMEA	Poly(2-methoxyethyl acrylate)
PNIPAM	Poly(*N*-isopropyl acrylamide)
POP	Polyoxypropylene
PVA	Poly(vinyl alcohol)
PVP	Poly(*N*-vinyl-2-pyrrolidone)

Monomers for copolymerization

AAG	Acrylamide glycolic acid
DMAEMA	2-(Dimethylamino)ethyl methacrylate
DMAPMA	*N*-[3-(Dimethylamino)propyl]methacrylamide
SMA	Sodium methacrylate
SSNa	Sodium 4-styrene sulfonate

Others

AMO	Amine-terminating Mannich oligomers
APS	Ammonium persulfate
APTMA	(3-Acrylamidopropyl)trimethylammonium
BP	Benzoyl peroxide
CNPs	Clay mineral nanoplatelets
CTAB	Cetyltrimethylammonium bromide
CV	Crystal violet
KPS	Potassium persulfate
LCST	Lower critical solution temperature
LDH	Layered double hydroxide
NMBA	*N*,*N*-Methylene-(bis)-acrylamide
SGPT	Sol–gel phase transition
TEMED	*N*,*N*,*N*′,*N*′-Tetramethylene diamine
TSPP	Tetrasodium diphosphate decahydrate
VPT	Volume phase transitions

Acknowledgements

The authors wish to acknowledge the financial support from the National Natural Scientific Foundation of China (21373185), the Distinguished Young Scholar Grants from the Natural Scientific Foundation of Zhejiang Province (ZJNSF, R4100436), ZJNSF (LQ12B03004), Zhejiang 151 Talents Project, and the projects (2010C14013 and 2009R50020-12) from Science and Technology Department of Zhejiang Provincial Government and the financial

support by the open fund from Key Laboratory of Clay Minerals of the Ministry of Land and Resources, China, (2014-K02) and Engineering Research Center of Non-metallic Minerals of Zhejiang Province (ZD2015k07), Zhejiang Institute of Geology and Mineral Resource, China, and the State Key Laboratory Breeding Base of Green Chemistry-Synthesis Technology, Zhejiang University of Technology (GCTKF2014006). CHZ conceived the work. LZZ drew or adapted illustrations and made the drafts which were substantially revised or rewritten by CHZ numerous times. HW made some corrections twice and JW made minor corrections once. The authors also feel grateful to anonymous reviewers for their comments and suggestions, which are much helpful for us to improve the manuscript.

References

1 K. Kabiri, H. Omidian, M. Zohuriaan-Mehr and S. Doroudiani, *Polym. Compos.*, 2011, **32**, 277–289.
2 J. Jagur-Grodzinzki, *Polym. Adv. Technol.*, 2010, **21**, 27–47.
3 T. Sun, T. Kurokawa, S. Kuroda, A. B. Ihsan, T. Akasaki, K. Sato, M. A. Haque, T. Nakajima and J. Gong, *Nat. Mater.*, 2013, **12**, 932–937.
4 J. Kopeček and J. Yang, *Polym. Int.*, 2007, **56**, 1078–1098.
5 L. A. Estroff and A. D. Hamilton, *Chem. Rev.*, 2004, **104**, 1201–1217.
6 E. A. Appel, M. W. Tibbitt, M. J. Webber, B. A. Mattix, O. Veiseh and R. Langer, *Nat. Commun.*, 2015, **6**, 6295.
7 L. Liu, X. Tang, Y. Wang and S. Guo, *Int. J. Pharm.*, 2011, **414**, 6–15.
8 M. Moriyama, N. Mizoshita, T. Yokota, K. Kishimoto and T. Kato, *Adv. Mater.*, 2003, **15**, 1335–1338.
9 A. R. Hirst, B. Escuder, J. F. Miravet and D. K. Smith, *Angew. Chem., Int. Ed.*, 2008, **47**, 8002–8018.
10 M. K. Shin, G. M. Spinks, S. R. Shin, S. I. Kim and S. J. Kim, *Adv. Mater.*, 2009, **21**, 1712–1715.
11 X. Liu, T. Zhou, Z. Du, Z. Wei and J. Zhang, *Soft Matter*, 2011, **7**, 1986–1993.
12 L. Xia, R. Xie, X. Ju, W. Wang, Q. Chen and L. Chu, *Nat. Commun.*, 2013, **4**, 2226–2236.
13 K. Adesanya, E. Vanderleyden, A. Embrechts, P. Glazer, E. Mendes and P. Dubruel, *Appl. Polym. Sci.*, 2014, **131**, 41195–41203.
14 S. Varghese, A. K. Lele, D. Srinivas, M. Sastry and R. A. Mashelka, *Adv. Mater.*, 2001, **13**, 1544–1548.
15 D. G. Barrett, D. E. Fullenkamp, L. He, N. Holten-Andersen, K. Y. C. Lee and P. B. Messersmith, *Adv. Funct. Mater.*, 2013, **23**, 1111–1119.
16 P. D. Thornton, R. J. Mart and R. V. Ulijn, *Adv. Mater.*, 2007, **19**, 1252–1256.
17 T. S. Anirudhan and A. R. Tharun, *Chem. Eng. J.*, 2012, **181**, 761–769.
18 M. J. Zohuriaan-Mehr, H. Omidian, S. Doroudiani and K. Kabiri, *J. Mater. Sci.*, 2010, **45**, 5711–5735.
19 A. Musetti, K. Paderni, P. Fabbri, A. Pulvirenti, M. Al-Moghazy and P. Fava, *J. Food Sci.*, 2014, **79**, 577–582.
20 L. Dong, A. K. Agarwal, D. J. Beebe and H. R. Jiang, *Nature*, 2006, **442**, 551–554.
21 D. J. Beebe, J. S. Moore, J. M. Bauer, Q. Yu, R. H. Liu, C. Devadoss and B. H. Jo, *Nature*, 2000, **404**, 588–590.
22 G. Cirillo, F. P. Nicoletta, M. Curcio, U. G. Spizzirri, N. Picci and F. Iemma, *React. Funct. Polym.*, 2014, **83**, 62–69.
23 N. Sahiner and F. Seven, *Energy*, 2014, **71**, 170–179.
24 M. A. Alam, M. Takafuji and H. Ihara, *Polym. J.*, 2015, **46**, 293–300.
25 A. K. Gaharwar, N. A. Peppas and A. Khademhosseini, *Biotechnol. Bioeng.*, 2014, **111**, 441–453.
26 N. S. Satarkar, D. Biswal and J. Z. Hilt, *Soft Matter*, 2010, **6**, 2364–2371.
27 C. Zhou and J. Keeling, *Appl. Clay Sci.*, 2013, **74**, 3–9.
28 D. Zhang, C. Zhou, C. Lin, D. Tong and W. Yu, *Appl. Clay Sci.*, 2010, **50**, 1–11.
29 N. Iyi, Y. Ebina and T. Sasaki, *Langmuir*, 2008, **24**, 5591–5598.
30 J. N. Coleman, M. Lotya, A. O'Neill, S. D. Bergin, P. J. King and U. Khan, *Science*, 2011, **331**, 568–571.
31 V. Nicolosi, C. Manish, M. G. Kanatzidis, M. S. Strano and J. N. Coleman, *Science*, 2013, **340**, 1420–1438.
32 K. Haraguchi and T. Takehisa, *Adv. Mater.*, 2002, **14**, 1120–1124.
33 T. Huang, *Appl. Phys. A: Mater. Sci. Process.*, 2012, **107**, 905–909.
34 K. Haraguchi and H. J. Li, *Macromolecules*, 2006, **39**, 1898–1905.
35 J. Wang, L. Lin, Q. Cheng and L. Jiang, *Angew. Chem., Int. Ed.*, 2012, **51**, 4676–4680.
36 J. Ma, Y. Xu, Q. Zhang, L. Zha and B. Liang, *Colloid Polym. Sci.*, 2007, **285**, 479–484.
37 A. B. Imran, T. Seki and Y. Takeoka, *Polym. J.*, 2010, **42**, 839–851.
38 W. F. Lee and L. L. Jou, *J. Appl. Polym. Sci.*, 2004, **94**, 74–82.
39 N. Y. Kostina, S. Sharifi, A. de los Santos Pereira, J. Michálek, D. W. Grijpmabc and C. Rodriguez-Emmenegger, *J. Mater. Chem. B*, 2013, **1**, 5644–5650.
40 S. Miyazaki, H. Endo, T. Karino, K. Haraguchi and M. Shibayama, *Macromolecules*, 2007, **40**, 4287–4295.
41 K. Haraguchi and D. Varade, *Polymer*, 2014, **55**, 2496–2500.
42 F. H. A. Rodrigues, A. G. B. Pereira, A. R. Fajardo and E. C. Muniz, *J. Appl. Polym. Sci.*, 2013, **128**, 3480–3489.
43 D. A. Young and D. E. Smith, *J. Phys. Chem. B*, 2000, **104**, 9163–9170.
44 C. C. Wang, L. C. Juang, C. K. Lee, T. C. Hsu, J. F. Lee and H. P. Chao, *J. Colloid Interface Sci.*, 2004, **280**, 27–35.
45 J. Zhao, A. B. Morgan and J. D. Harris, *Polymer*, 2005, **46**, 8641–8660.
46 T. R. Guimarães, T. de Camargo Chaparro, F. D'Agosto, M. Lansalot, A. M. D. Santos and E. Bourgeat-Lami, *Polym. Chem.*, 2014, **5**, 6611–6622.
47 C. C. Chu, M. L. Chiang, C. M. Tsai and J. J. Lin, *Macromolecules*, 2005, **38**, 6240–6243.
48 P. Mongondry, T. Nicolai and J. F. Tassin, *J. Colloid Interface Sci.*, 2004, **275**, 191–196.

49 P. Chen, S. Xu, R. Wu, J. Wang, R. Gu and J. Du, *Appl. Clay Sci.*, 2013, **72**, 196–200.
50 Y. C. Wang, T. K. Huang, S. H. Tung, T. M. Wu and J. J. Lin, *Sci. Rep.*, 2013, **3**, 2621.
51 L. Xiong, X. Hu, X. Liu and Z. Tong, *Polymer*, 2008, **49**, 5064–5071.
52 K. Haraguchi, *Polym. J.*, 2011, **43**, 223–241.
53 P. Li, N. H. Kim, D. Hui, K. Y. Rhee and J. H. Lee, *Appl. Clay Sci.*, 2009, **46**, 414–417.
54 X. Hu, L. Xiong, T. Wang, Z. Lin, X. Liu and Z. Tong, *Polymer*, 2009, **50**, 1933–1938.
55 M. Fukasawa, T. Sakai, U. Chung and K. Haraguchi, *Macromolecules*, 2010, **43**, 4370–4378.
56 H. Takeno and W. Nakamura, *Colloid Polym. Sci.*, 2013, **291**, 1393–1399.
57 M. J. A. Oliveira, E. O. Silva, L. M. A. Braz, R. Maia, V. S. Amato, A. B. Lugão and D. F. Parra, *Radiat. Phys. Chem.*, 2014, **94**, 194–198.
58 Q. Wang, J. L. Maynar, M. Yoshida, E. Lee, M. Lee, K. Okuro, K. Kinbara and T. Aida, *Nature*, 2010, **463**, 339–343.
59 M. Sirousazar, M. Kokabi and Z. M. Hassan, *J. Biomater. Sci., Polym. Ed.*, 2011, **22**, 1023–1033.
60 C. W. Chang, A. van Spreeuwel, C. Zhang and S. Varghese, *Soft Matter*, 2010, **6**, 5157–5164.
61 A. K. Gaharwar, V. Kishore, C. Rivera, W. Bullock, C. J. Wu, O. Akkus and G. Schmidt, *Macromol. Biosci.*, 2012, **12**, 779–793.
62 E. Loizou, P. Butler, L. Porcar and G. Schmidt, *Macromolecules*, 2006, **39**, 1614–1619.
63 A. Nelson and T. Cosgrove, *Langmuir*, 2004, **20**, 2298–2304.
64 K. Haraguchi and H. J. Li, *J. Polym. Sci., Part B: Polym. Phys.*, 2009, **47**, 2328–2340.
65 O. Okay and W. Oppermann, *Macromolecules*, 2007, **40**, 3378–3387.
66 M. Shen, L. Li, Y. Sun, J. Xu, X. Guo and R. K. Prud' home, *Langmuir*, 2014, **30**, 1636–1642.
67 M. Irani, H. Ismail and Z. Ahmad, *Polym. Test.*, 2013, **32**, 502–512.
68 P. Li, Siddaramaiah, N. H. Kim, S. B. Heo and J. H. Lee, *Composites, Part B*, 2008, **39**, 756–763.
69 K. Haraguchi, T. Takehisa and S. Fan, *Macromolecules*, 2002, **35**, 10162–10171.
70 B. Urbano and B. L. Rivas, *Polym. Bull.*, 2011, **67**, 1823–1836.
71 Y. Wang, W. Wang and A. Wang, *Chem. Eng. J.*, 2013, **228**, 132–139.
72 K. Kabiri, H. Mirzadeh, M. J. Zohuriaan-Mehra and M. Daliric, *Polym. Int.*, 2009, **58**, 1252–1259.
73 K. Kabiri, H. Mirzadeh and M. J. Zohuriaan-Mehra, *J. Appl. Polym. Sci.*, 2010, **116**, 2548–2556.
74 S. G. Starodoubtsev, A. A. Ryabova, A. R. Khokhlov, G. Allegra, A. Famulari and S. V. Meille, *Langmuir*, 2003, **19**, 10739–10746.
75 M. Liu, W. Li, J. Rong and C. Zhou, *Colloid Polym. Sci.*, 2012, **290**, 895–905.
76 Y. Yagci, S. Jockusch and N. J. Turro, *Macromolecules*, 2010, **43**, 6245–6260.
77 H. Kazutoshi and T. Tetsuo, *Macromolecules*, 2010, **43**, 4294–4299.
78 C. Altinkok, T. Uyar, M. A. Tasdelen and Y. Yagci, *J. Polym. Sci., Part A: Polym. Chem.*, 2011, **49**, 3658–3663.
79 S. Tamesue, M. Ohtani, K. Yamada, Y. Ishida, M. Spruell, N. A. Lynd, C. J. Hawker and T. Aida, *J. Am. Chem. Soc.*, 2013, **135**, 15650–15655.
80 A. S. Weingarten, R. V. Kazantsev, L. C. Palmer, M. McClendon, A. R. Koltonow, A. P. S. Samuel, D. J. Kiebala, M. R. Wasielewski and S. I. Stupp, *Nat. Chem.*, 2014, **6**, 964–970.
81 F. Song, L. Zhang, J. Shi and N. Li, *Colloids Surf., B*, 2010, **81**, 486–491.
82 C. M. Hassan and N. A. Peppas, *Adv. Polym. Sci.*, 2000, **153**, 37–65.
83 M. Sirousazar, M. Kokabi and Z. M. Hassan, *J. Appl. Polym. Sci.*, 2012, **123**, 50–58.
84 M. Kokabi, M. Sirousazar and Z. M. Hassan, *Eur. Polym. J.*, 2007, **43**, 773–781.
85 S. M. Ibrahim and A. A. El-Naggar, *J. Thermoplast. Compos. Mater.*, 2012, **26**, 1332–1348.
86 N. Bitinis, M. Hernandez, R. Verdejo, J. M. Kenny and M. A. Lopez-Manchado, *Adv. Mater.*, 2011, **23**, 5229–5236.
87 K. Haraguchi, *Macromol. Symp.*, 2007, **256**, 120–130.
88 W. F. Lee and Y. T. Fu, *J. Appl. Polym. Sci.*, 2003, **89**, 3652–3660.
89 J. P. Maranchi, M. M. Trexler, Q. Guo and J. H. Elisseeff, *Int. Mater. Rev.*, 2014, **59**, 264–296.
90 A. Zadražil and F. Štěpánek, *Colloids Surf., A*, 2010, **372**, 115–119.
91 N. Patil, J. Soni, N. Ghosh and P. De, *J. Phys. Chem. B*, 2012, **116**, 13913–13921.
92 M. Shibayama, T. Karino, S. Miyazaki, S. Okabe, T. Takehisa and K. Haraguchi, *Macromolecules*, 2005, **38**, 10772–10781.
93 K. Haraguchi, *Curr. Opin. Solid State Mater. Sci.*, 2007, **11**, 47–54.
94 P. Kujawa and F. M. Winnik, *Macromolecules*, 2001, **34**, 4130–4135.
95 K. Murata and K. Haraguchi, *J. Mater. Chem.*, 2007, **17**, 3385–3388.
96 Y. Liu, M. Zhu, X. Liu, W. Zhang, B. Sun, Y. Chen and H. J. P. Adlerb, *Polymer*, 2006, **47**, 1–5.
97 K. Haraguchi, R. Farnworth, A. Ohbayashi and T. Takehisa, *Macromolecules*, 2003, **36**, 5732–5741.
98 E. Helvacıoğlu, V. Aydın, T. Nugay, N. Nugay, B. G. Uluocak and S. Şen, *J. Polym. Res.*, 2011, **18**, 2341–2350.
99 M. Zhu, Y. Liu, B. Sun, W. Zhang, X. Liu, H. Yu, Y. Zhang, D. Kuckling and H. J. P. Adler, *Macromol. Rapid Commun.*, 2006, **27**, 1023–1028.
100 J. Nie, B. Du and W. Oppermann, *Macromolecules*, 2005, **38**, 5729–5736.
101 P. Schexnailder, E. Loizou, L. Porcar, P. Butler and G. Schmidt, *Phys. Chem. Chem. Phys.*, 2009, **11**, 2760–2766.
102 A. K. Gaharwar, C. P. Rivera, C. J. Wu and G. Schmidt, *Acta Biomater.*, 2011, **7**, 4139–4148.
103 M. Liu, Y. Ishida, Y. Ebina, T. Sasaki, T. Hikima, M. Takata and T. Aida, *Nature*, 2015, **517**, 68–72.

104 V. Can, S Abdurrahmanoglu and O. Okay, *Polymer*, 2007, **48**, 5016–5023.
105 H. Ren, M. Zhu and K. Haraguchi, *Macromolecules*, 2011, **44**, 8516–8526.
106 J. Zhang, L. Wang and A. Wang, *Ind. Eng. Chem. Res.*, 2007, **46**, 2497–2502.
107 Y. Xiang, Z. Peng and D. Chen, *Eur. Polym. J.*, 2006, **42**, 2125–2132.
108 J. Yi and L. Zhang, *Eur. Polym. J.*, 2007, **43**, 3215–3221.
109 Z. Darvishi, K. Kabiri, M. J. Zohuriaan-Mehr and A. Morsali, *J. Appl. Polym. Sci.*, 2011, **120**, 3453–3459.
110 H. Kaşgöz, A. Durmus and A. Kaşgöz, *Polym. Adv. Technol.*, 2008, **19**, 213–220.
111 J. Aalaie, E. Vasheghani-Farahani, A. Rahmatpour and M. A. Semsarzadeh, *Eur. Polym. J.*, 2008, **44**, 2024–2031.
112 W. Zhang, W. Luo and Y. Fang, *Mater. Lett.*, 2005, **59**, 2876–2880.
113 E. Al, G. Güçlü, T. B. yim, S. Emik and S. Özgümüş, *J. Appl. Polym. Sci.*, 2008, **109**, 16–22.
114 X. Xia, J. Yih, N. A. D'Souza and Z. Hu, *Polymer*, 2003, **44**, 3389–3393.
115 A. Li, A. Wang and J. Chen, *Appl. Polym. Sci.*, 2004, **92**, 1596–1603.
116 J. Zhang and A. Wang, *React. Funct. Polym.*, 2007, **67**, 737–745.
117 S. K. Patra and S. K. Swain, *J. Appl. Polym. Sci.*, 2011, **120**, 1533–1538.
118 K. Haraguchi and H. J. Li, *Angew. Chem., Int. Ed.*, 2005, **44**, 6500–6504.
119 K. Haraguchi, *Colloid Polym. Sci.*, 2011, **289**, 455–473.
120 C. Yao, Z. Liu, C. Yang, W. Wang, X. Ju, R. Xie and L. Chu, *Adv. Funct. Mater.*, 2015, **25**, 2980–2991.
121 R. A. Frimpong, S. Fraser and J. Z. Hilt, *J. Biomed. Mater. Res., Part A*, 2006, **10**, 1–6.
122 Q. Yang, N. Adrus, F. Tomicki and M. Ulbricht, *J. Mater. Chem.*, 2011, **21**, 2783–2811.
123 K. Haraguchi, K. Murata and T. Takehisa, *Macromolecules*, 2012, **45**, 385–391.
124 Y. Satokawa, T. Shikata, F. Tanaka, X. Qiu and F. M. Winnik, *Macromolecules*, 2009, **42**, 1400–1403.
125 L. W. Xia, R. Xie, X. J. Ju, W. Wang, Q. Chen and L. Y. Chu, *Nat. Commun.*, 2013, **4**, 2226–2236.
126 T. S. Anirudhan and S. Sandeep, *New J. Chem.*, 2011, **35**, 2869–2876.
127 Y. Li, D. Maciel, H. Tom as, J. Rodrigues, H. Ma and X. Shi, *Soft Matter*, 2011, **7**, 6231–6238.
128 H. Li, R. Wu, J. Zhu, P. Guo, W. Ren, S. Xu and J. Wang, *J. Polym. Sci., Part B: Polym. Phys.*, 2015, **53**, 876–884.
129 M. Boruah, M. Mili, S. Sharma, B. Gogoi and S. K. Dolui, *Polym. Compos.*, 2014, **36**, 34–41.
130 H. Zhang, J. Li, H. Cui, H. Li and F. Yang, *Chem. Eng. J.*, 2015, **259**, 814–819.
131 G. R. Mahdavinia, B. Massoumi, K. Jalili and G. Kiani, *J. Polym. Res.*, 2012, **19**, 9947–9959.
132 H. Kaşgöz, A. Durmus and A. Kaşgöz, *Polym. Adv. Technol.*, 2008, **19**, 213–220.
133 J. Yi and L. Zhang, *Bioresour. Technol.*, 2008, **99**, 2182–2186.
134 A. S. Ozcan, B. Erdem and A. J. Ozcan, *J. Colloid Interface Sci.*, 2004, **280**, 44–54.
135 L. Wu, M. Ohtani, S. Tamesue, Y. Ishida and T. Aida, *J. Polym. Sci., Part A: Polym. Chem.*, 2014, **52**, 839–847.
136 G. Güçlü, E. Al, S. Emik, T. B. İyim, S. Özgümüş and M. Özyürek, *Polym. Bull.*, 2010, **65**, 333–346.
137 G. R. Mahdavinia, H. Aghaie, H. Sheykhloie, M. T. Vardini and H. Etemadi, *Polymer*, 2013, **98**, 358–365.
138 L. Zhang, Y. Zhou and Y. Wang, *J. Chem. Technol. Biotechnol.*, 2006, **81**, 799–804.
139 K. V. Rao, A. Jain and S. J. George, *J. Mater. Chem. C*, 2014, **2**, 3055–3064.
140 T. Vermonden, R. Censi and W. E. Hennink, *Chem. Rev.*, 2012, **112**, 2853–2888.
141 D. Depan, A. P. Kumar and R. P. Singh, *Acta Biomater.*, 2009, **5**, 93–100.
142 T. Takahashi, Y. Yamada, K. Kataoka and Y. J. Nagasaki, *J. Controlled Release*, 2005, **107**, 408–416.
143 J. I. Dawson, J. M. Kanczler, X. B. Yang, G. S. Attard and R. O. C. Oreffo, *Adv. Mater.*, 2011, **23**, 3304–3308.
144 C. Wu and G. Schmidt, *Rapid Commun.*, 2009, **30**, 1492–1497.
145 C. Viseras, C. Aguzzi, P. Cerezo and M. C. Bedmar, *Mater. Sci. Technol.*, 2008, **24**, 1020–1026.
146 T. S. Anirudhan and S. J. Sandeep, *Mater. Chem.*, 2012, **22**, 12888–12899.
147 M. Boruah, P. Gogoi, A. K. Manhar, M. Khannam, M. Mandal and S. K. Dolui, *RSC Adv.*, 2014, **4**, 3865–43873.
148 B. D. Kevadiya, G. V. Joshi, H. M. Mody and H. C. Bajaj, *Appl. Clay Sci.*, 2011, **52**, 364–367.
149 B. D. Kevadiya, R. R. Pawar, S. Rajkumar, R. Jog, Y. K. Baravalia, H. Jivrajani, N. Chotai, N. R. Sheth and H. C. Bajaj, *Biochem. Biophys.*, 2013, **1**, 43–60.
150 D. Liu, T. Wang, X. Liu and Z. Tong, *Biopolymers*, 2013, **101**, 58–65.
151 P. J. Schexnailder, A. K. Gaharwar, R. L. Bartlett, B. L. Seal and G. Schmidt, *Macromol. Biosci.*, 2010, **10**, 1416–1423.
152 G. Ozkoc, S. Kemaloglu and M. Quaedflieg, *Polym. Compos.*, 2010, **31**, 674–683.
153 H. Zhuang, J. Zheng, H. Gao and K. De Yao, *J. Mater. Sci.: Mater. Med.*, 2007, **18**, 951–957.
154 J. L. Drury and D. J. Mooney, *Biomaterials*, 2003, **24**, 4337–4351.
155 Q. Jin, P. Schexnailder, A. K. Gaharwar and G. Schmidt, *Macromol. Biosci.*, 2009, **9**, 1028–1035.
156 H. L. Lim, J. C. Chuang, T. Tran, A. Aung, G. Arya and S. Varghese, *Adv. Funct. Mater.*, 2011, **21**, 55–63.
157 K. Haraguchi, T. Takehisa and M. Ebato, *Biomacromolecules*, 2006, **7**, 3267–3275.
158 N. Kotobuki, K. Murata and K. Haraguchi, *J. Biomed. Mater. Res., Part A*, 2013, **101**, 537–546.
159 A. K. Gaharwar, P. Schexnailder, V. Kaul, O. Akkus, D. Zakharov, S. Seifert and G. Schmidt, *Adv. Funct. Mater.*, 2010, **20**, 429–436.

160 K. Haraguchi, S. Masatoshi, N. Kotobuki and K. Murata, *J. Biomater. Sci., Polym. Ed.*, 2011, **22**, 2389–2406.
161 N. An, C. Zhou, X. Zhuang, D. Tong and W. Yu, *Appl. Clay Sci.*, 2015, **114**, 283–296.
162 D. Gao, R. B. Heimann, J. Lerchner, J. Seidel and G. Wolf, *J. Mater. Sci.*, 2001, **36**, 4567–4571.
163 M. Ikeda, T. Yoshii, T. Matsui, T. Tanida, H. Komatsu and I. Hamachi, *J. Am. Chem. Soc.*, 2011, **133**, 1670–1673.
164 Q. Shi, Q. Li, D. Shan, Q. Fan and H. Xue, *Mater. Sci. Eng., C*, 2008, **28**, 1372–1375.
165 S. Y. Lin, K. S. Chen and L. Run-Chu, *Biomaterials*, 2001, **22**, 2999–3004.
166 T. S. Anirudhan, S. S. Gopal and S. Sandeep, *Appl. Clay Sci.*, 2014, **88–89**, 151–158.
167 M. Shen, L. Li, Y. Sun, J. Xu, X. Guo and R. K. Prud'homme, *Langmuir*, 2014, **30**, 1636–1642.

